frontiers | Frontiers in Earth Science

TYPE Original Research
PUBLISHED 10 September 2025
DOI 10.3389/feart.2025.1605844

OPEN ACCESS

EDITED BY
Jungrack Kim,
University of Seoul, Republic of Korea

REVIEWED BY
Tejpal Singh,
Council of Scientific and Industrial Research (CSIR), India
Riheb Hadji,
University Ferhat Abbas of Setif, Algeria
Imad Mahmood Ghafor,
University of Sulaymaniyah, Iraq
Yandong Hou,
Chinese Academy of Sciences (CAS), China

*CORRESPONDENCE
Ulambadrakh Khukhuudei,
ulambadrakh@num.edu.mn

RECEIVED 04 April 2025
ACCEPTED 18 August 2025
PUBLISHED 10 September 2025

CITATION
Enkhbold A, Khukhuudei U, Seong YB, Yadamsuren G, Batbold B, Davaasuren D, Ganbat S, Tsedevdorj S-O, Bold B, Badarch D and Ganbold B (2025) Tectonic geomorphology of the lake depressions in the Mongolian Altai mountains, western Mongolia.
Front. Earth Sci. 13:1605844.
doi: 10.3389/feart.2025.1605844

Tectonic geomorphology of the lake depressions in the Mongolian Altai mountains, western Mongolia

Altanbold Enkhbold[1], Ulambadrakh Khukhuudei[2,3]*, Yeong Bae Seong[4], Gansukh Yadamsuren[5], Batzorig Batbold[1], Davaadorj Davaasuren[1], Shuukhaaz Ganbat[6], Ser-Od Tsedevdorj[7], Bat Bold[8], Daariimaa Badarch[8] and Byambabayar Ganbold[1]

[1]Laboratory of Geopedology, Department of Geography, School of Arts and Sciences, National University of Mongolia, Ulaanbaatar, Mongolia, [2]Research Center of Geology and Mineral Resources, School of Arts and Sciences, National University of Mongolia, Ulaanbaatar, Mongolia, [3]Center for Global Tectonics, School of Earth Sciences and State Key Laboratory for Geological Processes and Mineral Resources, China University of Geosciences, Wuhan, China, [4]Department of Geography Education, Korea University, Seoul, Republic of Korea, [5]Department of Ecology, Agroecology School, Mongolian University of Life Sciences, Ulaanbaatar, Mongolia, [6]Division of Natural System, Institute of Nature and Environmental Technology, Kanazawa University, Kanazawa, Japan, [7]Department of Geography, School of Mathematics and Natural Sciences, Mongolian National University of Education, Ulaanbaatar, Mongolia, [8]Department of Geology-Geophysics, School of Arts and Sciences, National University of Mongolia, Ulaanbaatar, Mongolia

This study explores the tectonic geomorphology of lake depressions in the Mongolian Altai Mountains (MAM), focusing on three prominent lakes: Tolbo, Achit, and Uureg. These lakes are situated within tectonically active zones in the westernmost part of Mongolia, providing valuable insights into the interplay between geological processes and geomorphological evolution. The study investigates the structural characteristics and faults influencing lake depressions, utilizing satellite imagery, morphometric analysis, and geomorphological criteria interpretation. The morphometric analysis reveals significantly high HI (%) values for the Uureg, Achit, and Tolbo lake depressions, suggesting active tectonic movements in these regions. Additionally, the Smf, Bs, RSl, and Re indices support the evidence of ongoing tectonic processes. Since the northern MAM are located within a transpressional stress regime, the associated basins are expected to reflect this tectonic setting. Accordingly, all intermontane basins in the region are characterized as half-ramp, remnant low, or ramp basins. Each depression is shaped by different fault regimes, including thrust, strike-slip, and tilted thrust faults. These depressions are controlled by neotectonic processes associated with the Indian–Eurasian plate collision. Their dynamic nature underscores their significance as key tectonic features in the MAM. This case study deepens our understanding of the dynamic interplay between tectonics and lake depression formation in seismically active regions. It contributes valuable insights into the geomorphological evolution of mountainous landscapes.

KEYWORDS

tectonic geomorphology, morphometric analysis, lake depression, geomorphological criteria interpretation, Khovd zone, Tsagaan Shuvuut fault, Tolbo Nuur fault

1 Introduction

Understanding the formation and evolution of lake depressions is essential for analyzing lake basin morphology, structure, and long-term landscape development (Dietze et al., 2010). This process is influenced by factors such as rock composition, structural configuration, tectonic uplift and subsidence, and regional climate conditions (Leeder, 2011; Lehner, 2024; Huang et al., 2024). In particular, the relationship between faults and depressions is crucial for determining the structural origin of lakes and distinguishing between tectonic, glacial, or mixed-genesis basins (Dietze et al., 2010; Faghih et al., 2012; Enkhbold et al., 2022a, b, c). The initial geomorphic structure of lake basins strongly influences their hydrological dynamics and ecological functions (Dietze et al., 2010; Schallenberg et al., 2013), making tectonic interpretation vital for sustainable ecosystem management (Enkhbold et al., 2021; Jones et al., 2022).

The MAM region is characterized by an active tectonic setting and a complex network of fault-controlled depressions (Cunningham, 2005; Nissen et al., 2009a; Emanov et al., 2012; Enkhbold et al., 2024a; Ramel et al., 2025). These tectonic features have governed the geomorphic configuration of the area, resulting in closed-basin lakes that are highly sensitive to both endogenic and exogenic processes. Understanding the structural and morphometric characteristics of these lake basins is thus essential for interpreting long-term environmental dynamics, including lake formation, expansion, and potential desiccation events.

In Central Asia, lake distribution and basin morphologies have been shaped not only by tectonic processes but also by glacial and post-glacial climatic conditions (Grunert et al., 2000; Lehmkuhl et al., 2018a; Klinge et al., 2021; Demberel et al., 2024; Lehmkuhl et al., 2024). However, the underlying tectonic framework often dictates where glacial processes act, influencing basin depth, orientation, and sediment accumulation (Dietze et al., 2010; Lehmkuhl et al., 2018a).

The Cenozoic mountain belts of Central Asia provide key insights into intracontinental deformation processes (Walker et al., 2007; Yarmolyuk et al., 2011; Khukhuudei et al., 2022; Khukhuudei et al., 2024). Mongolia, centrally located within the Eurasian continent, lies in a zone of complex neotectonic activity driven by far-field stresses from the India–Asia collision (Molnar and Tapponnier, 1975; Tapponnier and Molnar, 1979; Copley and McKenzie, 2007). In this context, the Mongolian Altai Mountains (MAM) represent an important region for investigating the geomorphic consequences of active tectonism, where large depressions have formed as a result of transpressional deformation since the Late Cenozoic (De Grave and Buslov, 2007; Jolivet et al., 2007; Walker et al., 2007; Ha et al., 2023).

The MAM, Although previous research has revealed a multifaceted Cenozoic deformation history involving shortening, strike-slip, and extensional regimes, precise age constraints on fault formation and reactivation remain scarce due to limited geochronological data. According to previous studies, the faults in the Mongolian Altai originated during significant Neogene uplift, and Quaternary fault activity has continued to the present (Baljinnyam, 1993; Cunningham et al., 2003; Cunningham, 2005; Bayasgalan et al., 2005; De Grave and Buslov, 2007; Walker et al., 2006; Walker et al., 2007; Nissen et al., 2009ab; Emanov et al., 2012; Ha et al., 2023; Enkhbold et al., 2024a; Trifonov et al., 2024; Ramel et al., 2025).

The MAM are characterized by major thrust and strike-slip fault systems (Baljinnyam, 1993; Bayasgalan et al., 1999b; Nissen et al., 2009b), which have governed the formation and evolution of prominent lake depressions such as Uureg, Achit, and Tolbo (Tserensodnom, 2000; Agatova and Nepop, 2019). Although many lakes in the region are glacially fed (Walther et al., 2024; Li et al., 2025), their underlying basins are structurally controlled, with tectonic faulting playing a primary role in their initial development (Enkhbold et al., 2024a; Trifonov et al., 2024; Ramel et al., 2025).

Notably, fault-related vertical displacement has shaped the depth, extent, and orientation of these depressions. For instance, a new fault segment formed in the Uureg Lake basin following a magnitude-7 earthquake in 1970, altering river inflow patterns and generating new lake terraces (Emanov et al., 2012). These tectonic dynamics have implications not only for landscape morphology but also for the interpretation of sedimentary records and paleoclimate proxies. While previous studies have reconstructed sediment chronologies for Achit and Tolbo Lakes (Zhang et al., 2023; Hu et al., 2024; Zhang, 2012; Huang et al., 2018; Chen et al., 2023), they often underrepresent the geomorphological controls underlying these records. The chronological records derived from lake sediments mainly reflect variations in paleoclimate.

Given the need for a clearer understanding of tectonic controls on lake basin formation in the MAM, this study applies satellite-based morphometric analysis to assess fault structures in the Uureg, Achit, and Tolbo lake depressions. Although no direct chronological data are included, the study provides critical structural insights that may serve as a baseline for future interdisciplinary research on tectonic-limnological interactions and paleoclimate reconstruction.

This study aims to identify and characterize the tectonic structures and morphometric configurations of the Uureg, Achit, and Tolbo lake depressions in the MAM, in order to assess how active fault systems have shaped the origin and evolution of these intermontane basins.

2 Regional settings

The Altai Mountains stretch from the northwest to the southeast (45–52°N, 89–94°E), crossing the borders of Mongolia, China, Russia, and Kazakhstan (Khil'ko and Kurushin, 1982; Strand et al., 2022). As one of the most prominent mountain systems in Central Asia, the Altai Mountains serve as a significant ecological and geological boundary, separating distinct environmental zones (Lehmkuhl, 2016; Khukhuudei et al., 2024). Extending across regions of Mongolia, China, Russia, and Kazakhstan, this mountain range plays a crucial role in regulating regional climate patterns by acting as a barrier to atmospheric circulation and influencing precipitation distribution (Strand et al., 2022). The Altai Mountains form the headwaters of several major rivers, significantly contributing to the hydrological systems of central Asia (Lehmkuhl, 2016; Agatova and Nepop, 2019; Yembuu, 2021). This hydrological system is fundamental in maintaining the network of large lakes located in the continental interior, offering crucial support for the region's ecological integrity and hydrological balance (Klinge et al., 2021). Its diverse geology, shaped

by complex tectonic processes since the Oligocene, also provides key insights into the geomorphology and geological evolution of the region (Khukhuudei et al., 2024).

The Mongolian section of the Altai Mountains, known as the MAM, extends from the Tavan Bogd Mountains in the northwest and stretches southeastward, forming the largest mountain system in Mongolia with an elevation ranging from 3,000 to 4,000 m above sea level (Klinge et al., 2021; Enkhbold et al., 2024b). The MAM covers an area of 106,000 km^2, with a length of 800 km in an NW-SE direction and a width varying between 370 and 60 km (Khukhuudei et al., 2020). The MAM is composed of several mountain systems along a transpressional zone. The MAM transpressional zone is a tectonic region where horizontal compression and lateral shear occur, resulting in a transpressional regime (Cunningham et al., 1996). It is characterized by strike-slip and reverse faulting, which drive mountain-building processes, fault systems, and the uplift of the range (Cunningham, 2005; Khukhuudei et al., 2024). This zone plays a pivotal role in influencing the region's geomorphological and tectonic evolution, contributing to the development of landforms including mountains, basins, and fault systems (Cunningham, 1998). These landforms include the MAM, Khungiin Range-Deluun, Baatar Khairkhan-Sutai mountain, and Bairam-Kharkhiraa and Turgen ranges, separated by depressions and bounded by faults (Khil'ko and Kurushin, 1982).

This study focuses on three main lake depressions Tolbo, Achit, and Uureg located along a transect within the MAM mountain range, which is characterized by a distinctive geomorphological context. The research aims to validate satellite imagery, morphometric analysis, and geomorphological criteria for identifying fault lines within these depressions. It also explores the spatial distribution and interactions of these faults to enhance our understanding of the tectonic processes shaping the region (Figure 1).

The MAM experiences significant temperature fluctuations. The average winter air temperature is around −30 °C, while summer temperatures can reach up to +25 °C, resulting in a seasonal temperature variation of approximately 55 °C (Yembuu, 2021; Tsedevdorj et al., 2025). In the MAM, orographic precipitation occurs due to the influence of westerly winds, which contributes to the formation of permanent snow, glaciers, ice caps, lakes, and the main water sources for rivers (Klinge et al., 2021; Ghafor and Ahmad, 2021; Strand et al., 2022; Ghafor, 2022; Rashidi et al., 2023; Ghafor et al., 2023). The total amount of precipitation in the MAM is around 300 mm. In the vicinity of Uureg Lake, precipitation is 150–200 mm, near Achit Lake it is 100–150 mm, and around Tolbo Lake, it ranges from 200 to 250 mm (Yembuu, 2021). The hydrology of lakes in the MAM is closely linked to the region's precipitation patterns. Variations in precipitation influence meltwater, runoff, evaporation rates, and overall water levels, contributing to the hydrological dynamics of these lakes on both seasonal and interannual scales (Klinge et al., 2021; Yembuu, 2021; Strand et al., 2022).

The mountain system is essential for sustaining regional water resources, supporting habitats for rare and endemic species, and preserving ecological balance (Yembuu, 2021). Furthermore, due to its ethnogeographic characteristics and eco-tourism potential, the region presents considerable opportunities for the development of a variety of hydrology-based tourism activities (Tsedevdorj, 2019). Lakes in the MAM support diverse aquatic life, serve as crucial stopover points for migratory birds, and provide habitats for terrestrial species, such as the Mongolian gazelle and snow leopard, all of which depend on the health of the lake ecosystems (Laurie et al., 2010).

The geology of the Achit, Uureg, and Tolbo lake depressions is fundamental to this study, as it offers critical evidence of tectonic activity and basin formation processes that have directly shaped the development, morphology, and hydrological characteristics of these lakes.

Geologically, the MAM consists of four major stratigraphic sequences, ranging from the late Neoproterozoic to the Devonian (Dergunov et al., 1980; Tomurtogoo, 2014; Khukhuudei et al., 2020). The study area contains several ophiolitic complexes. Some fragmented ophiolites are primarily exposed in the axial part of the zone between the Tolbo Nuur and Khovd faults as a serpentinite mélange, gabbroids, and greenstone basalts, which are interpreted as remnants of paleo-oceanic crust (Tomurtogoo, 2014; Khukhuudei et al., 2020) (Figure 2).

The Uureg Lake depression is an endorheic lake located between the Western Bairam, Tsagaan Shuvuut, and Turgen Mountains in the MAM, with no outlet (Tserensodnom, 1971). The depression is encircled by elevated mountain ranges and lies at an approximate elevation of 1,400 m above sea level. North of Uureg Lake, the Tsagaanshuvuut zone occupies a small wedge-shaped area on the eastern side of the northwestern end of the MAM. According to Gavrilova (1975), the complex consists of late Neoproterozoic to lower Cambrian ophiolites, along with Paleozoic gneiss, amphibolite, migmatite, schist, quartzite, and metasandstone, which have been intruded by diorite and granodiorite, with a K–Ar age of 456 ± 23 Ma. Additionally, it contains Ordovician and Silurian andesite, tuff, sandstone, siltstone, and minor limestone with brachiopod fossils (Badarch et al., 2002). To the south of Uureg Lake, the Bayram zone is comprised of metamorphic complexes, featuring greenschists interlayered with thin bands of marble and quartzite in the lower strata. Flysch refers to a sequence of sedimentary rocks typically consisting of alternating layers of sandstone, shale, and mudstone. These formations are commonly associated with tectonically active, deep marine environments. In contrast, terrigenous sediments or rocks are derived from land through the weathering and erosion of continental rocks, as opposed to marine or volcanic sources (Izokh et al., 2010). The upper sections consist of terrigenous flysch, sills, flood basalts (Tomurtogoo, 2014), and intrusions of picrite, picrobasalt, and picrodolerite, with an age of 512 Ma (Izokh et al., 2010; Izokh et al., 2011).

The depression of Achit Lake was formed as a result of tectonic subsidence along faults, driven by extensional tectonics. This process created a structure that collects water. Similarly, the depression of Uureg Lake is shaped by faulting along the mountain boundary, with extensional forces creating a basin that continues to evolve due to ongoing tectonic activity. The depression of Tolbo Lake, influenced by faulting and flexural subsidence, reflects the tectonic movements of the surrounding mountain ranges, shaping the depression in which it is located.

The Uureg Lake depression is characterized by the widespread development of alluvial fans, formed through the accumulation

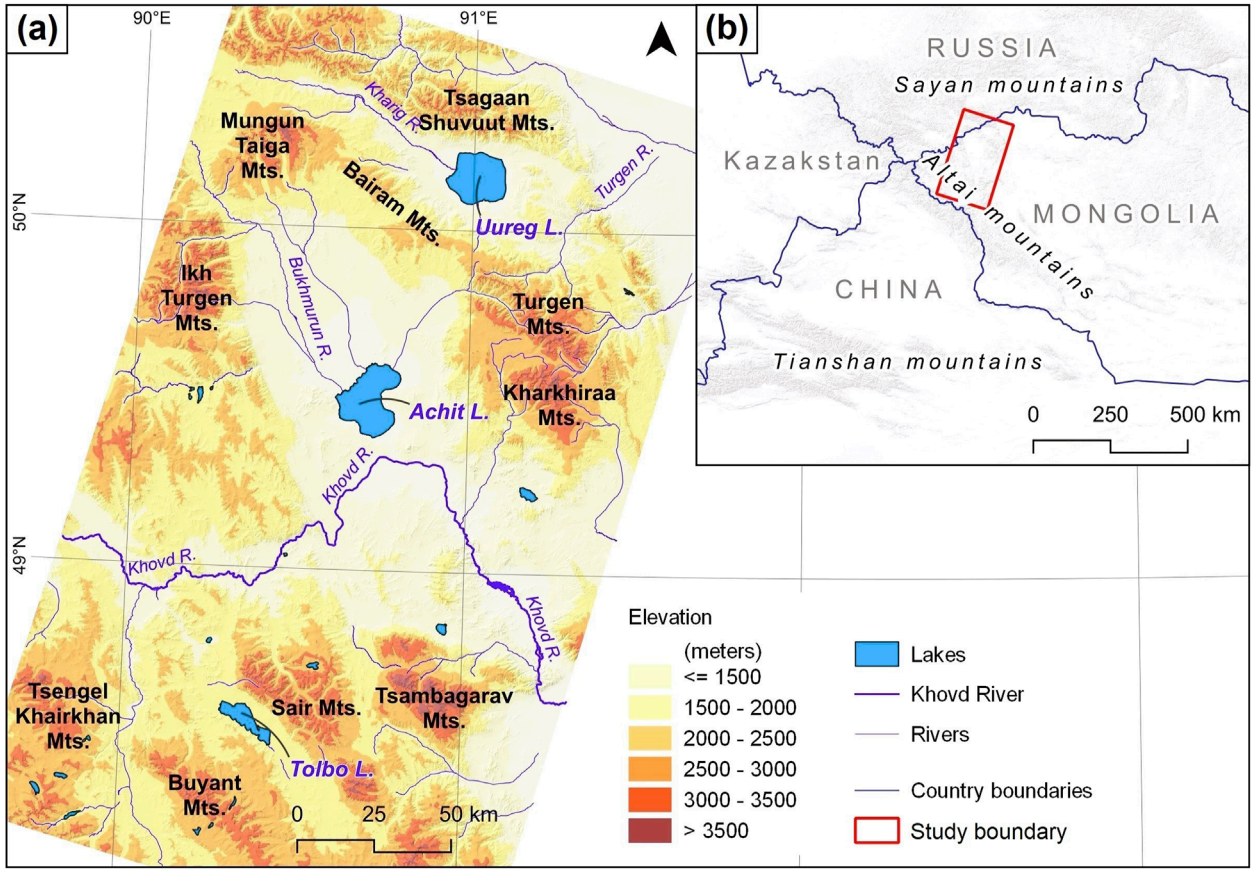

FIGURE 1
Locations of the Uureg, Achit, and Tolbo lakes within the study area **(a)**, Inset map depicting the major mountainous regions surrounding the study area **(b)**.

of lacustrine, fluvial, alluvial, and alluvial-colluvial deposits along the basin margins. One of the key geomorphic features is a well-defined terrace surrounding the lake, which provides evidence of historical hydrological fluctuations and shoreline displacement linked to climatic variability (Emanov et al., 2012). Several rivers and streams, such as Tsagaan Shuvuut, Tsagduul, and Kharig, flow into the lake, though most of them are ephemeral. The largest river with permanent flow, Kharigiin River, enters the lake from the southwest (Tserensodnom, 2000). Near the mouth of Kharigiin River, a swampy delta is formed.

Achit Lake depression is a large depression located between the major branches of the MAM, including the Siilkhem, Kharkhiraa, and Turgen Mountains. The geomorphological characteristics of the basin encompass an expansive valley situated between mountainous terrain. The western and northwestern parts are characterized by high mountains, while the eastern and southeastern areas are bordered by lower mountain ranges.

The area surrounding Achit Lake is characterized by lacustrine, fluvial, alluvial, and alluvial-colluvial deposits. In the western and eastern sectors, extensive alluvial fans, fed by catchments to the north, overlie marshy delta plains. Seasonal variations in lake levels induce shoreline migration, resulting in the formation of erosional scarps as well as depositional spits and berms along the deltas (Tserensodnom, 1971; Enkhbold et al., 2024a). By contrast, the southern and southeastern basin floors form a large equilibrium Surface of exposed bedrock, reflecting limited sediment cover and minimal contemporary fluvial deposition. The depression is nourished by water from several rivers and streams, including Tsagaan Nuur, Khatuu, Bukh, and Uliastai, all of which are generated from the surrounding mountains with meltwater (Tserensodnom, 1971; Tserensodnom, 2000). The excess water from Achit Lake flows eastward into the Khovd River.

The Khovd Zone is situated to the west of Achit Lake, along the eastern margin of the MAM. It consists of a series of thick, uniform terrigenous sandstone-siltstone beds ranging from the middle Cambrian to the lower Ordovician, with a noticeable lack of significant carbonate content. Following these are Silurian basalt, diabase, tuff, sandstone, and graptolitic shale (Dergunov, 1989). These rocks have been intruded by gabbro, diorite, granodiorite, and plagiogranite plutons, dated to 456–440 Ma through K–Ar dating (Gavrilova, 1975). The complex is present as fault-bounded disrupted blocks, thrust sheets, and tectonic slivers, with melanges in some areas containing ultramafic rocks, gabbro, and diabase. Overlapping assemblages include Devonian and Mississippian volcanic and sedimentary rocks, as well as Permian and Jurassic subalkaline granite plutons (Badarch et al., 2002).

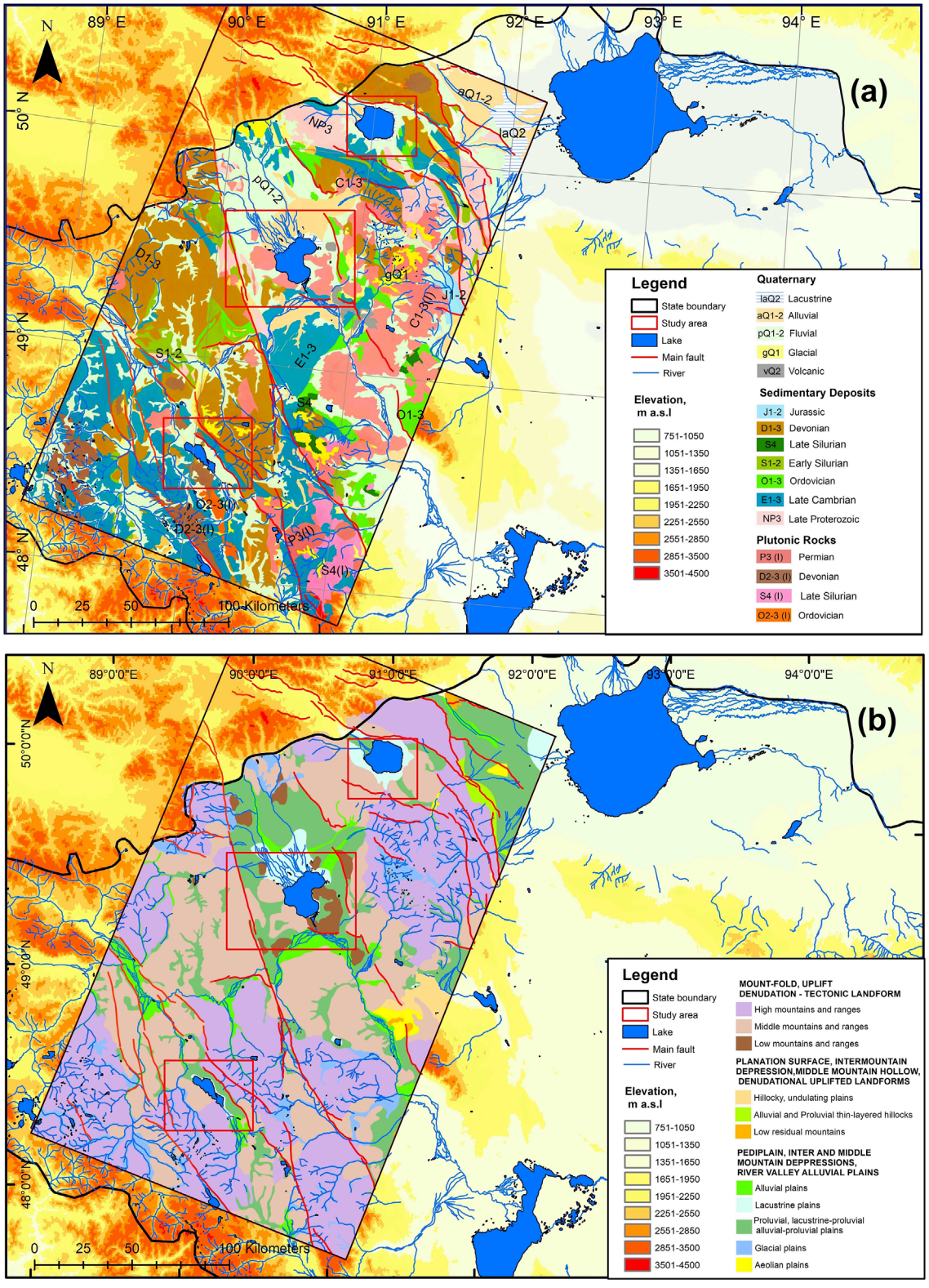

FIGURE 2
(a) Geological formations of the study area, Western Mongolia (modified after Khukhuudei et al., 2020), **(b)** Geomorphological characteristics of the study area (modified after Enkhbold et al., 2024c).

The Tolbo Lake depression is situated between the branches of the MAM, with an elevation ranging from 1,000 to 1,500 m, surrounded by major mountain ranges. The depression features a relatively flat central area but is delineated by large mountains. The Tolbo Lake depression, is located around the Deluun Range along with Devonian intrusions in the region (Carson et al., 2008; Khukhuudei et al., 2020). The Tolbo Lake fault, positioned at the southern foot of the Ridge, is bounded by Early Devonian rocks and Quaternary sediments (Baljinnyam, 1993).

The area surrounding Tolbo Lake is characterized by lacustrine, fluvial, alluvial, and alluvial-colluvial deposits. The northern and northeastern parts of the lake depression feature prominent alluvial fans, formed by the deposition of sediments transported by rivers and streams. These fans are created when water flowing from higher elevations loses velocity, causing materials like sand, gravel, and clay to accumulate. The fans are typically distinguished by gently inclined surfaces composed of stratified sediments. They are a clear indication of the dynamic interaction between water flow and sediment deposition processes. The presence of these alluvial fans offers valuable insights into the geomorphological evolution of the region and its hydrological regime (Klinge et al., 2021). In the southern section, the terrain consists of elevated lands with medium mountains (Lehmkuhl, 2016; Klinge et al., 2021). Numerous rivers and streams flow into the lake through mountain passes, and the lake drains its excess water through the Turgen River, eventually feeding into the Western Khovd tributary, the Omno River. During dry periods, when the lake level recedes, the lake loses its outlet and becomes endorheic. Despite this, the lake remains freshwater (Tserensodnom, 2000).

The elevation differences surrounding MAM lakes significantly influence erosion, sedimentation, and accumulation processes within their catchments. Rivers originating from high mountain areas incise deep valleys and contribute to the formation of alluvial fans, fan deltas, proluvium, and lake terraces along the lake shores. In contrast, the lower-lying zones are characterized by extensive lacustrine deposits. These lakes, in particular, exhibit well-developed landforms shaped by the surrounding rugged highlands.

3 Methodology

By integrating morphometric analysis, remote sensing mapping, and geomorphological criteria, we were able to identify tectonic faults as the primary factor shaping the morphological characteristics of the three lake depressions, as these methods collectively reveal linear alignments, structural patterns, and topographic anomalies indicative of fault activity.

A hypsometric cross-section covering a distance of 50–100 km was generated using 30-m resolution Digital Elevation Model (DEM) maps, integrated with bathymetric data from the lake depressions. Bathymetric data were sourced from published lake bathymetric maps (Tserensodnom, 2000), which were then digitized and incorporated into the DEM analysis to improve the precision of subaqueous topography within the hypsometric cross-sections. The hypsometric profile analysis provides strong evidence that fault activity has been a significant driver in shaping these depressions, as the elevation variations and topographic features align with the patterns of fault-induced deformation.

Morphometric measurements of the lakes were conducted during fieldwork in July 2024, utilizing tools such as a GPS device for precise location tracking, field photography for topographic analysis, and surface slope measurements to evaluate terrain characteristics.

3.1 Satellite image processing analysis

In this study, we utilized the Multi-resolution Valley Bottom Flatness (MrVBF) index, which classifies the degree of valley bottom flatness (Gallant and Dowling, 2003).

The MrVBF index is a geospatial analysis tool that combines two key parameters, flatness (inverse slope) and lowness (elevation percentile), to map valley bottoms within a specified circular neighborhood. These measures are both scaled from 0 to 1 and combined as fuzzy set memberships, following Kaufmann (1975), based on the FLAG method (Roberts et al., 1997; Gallant and Dowling, 2003; Malins and Metternicht, 2006). This method can analyze multiple scales enables it to capturing both broad and fine valley features. As a result, broad-scale flatness can dominate while preserving significant local variations. A location is identified as a valley bottom if it is sufficiently low and flat at the specified scale and flat at finer scales. The elevation percentile ranks a point's elevation relative to surrounding cells within a defined radius. The ratio of lower-elevation neighbors to the total is indicates the local position in the landscape, with low values suggesting low positions.

Differentiating valley bottoms from hillslopes is a crucial initial step in recognizing and analyzing sediment deposits for geomorphic studies (Davaasambuu et al., 2023). Firstly, the slope is calculated from a DEM, then transformed into flatness index (F from 0 to 1) using a non-linear function. Next, elevation percentile for the first step ($PCTL$) is determined with the three DEM cells. Elevation percentile is a metric that quantifies the elevation of a point relative to its surrounding cells within a specified radius. The ratio of lower-elevation neighbors to the total reflects the local position within the landscape, with lower values indicating positions at lower elevations. F_1 and the transformed elevation percentile act as membership functions with values greater than 0.5 indicating enough flatness or lowness to quality as a valley bottom. These steps are then repeated with a slope threshold for F_1 and a radius of 6 cells for $PCTL$. The results from steps one and two are then combined to create MrVBF.

We used SRTM a 30-m resolution from https://search.earthdata.nasa.gov/search. The calculating process was conducted in the MrVBF module of SAGA GIS (Conrad et al., 2015), it provides a dedicated tool for MrVBF calculation, optimized for performance and accuracy. It offers user-defined parameters for scale and resolution. A comparison of SAGA with other GIS platforms reveals its superiority in terms of flexibility in terrain analysis workflows. The platform's extensive utilization in geomorphological and hydrological studies is noteworthy, thereby establishing it as a reliable choice for valley bottom and fault-related feature detection. To ensure full coverage of the study area, Landsat images from path 142, rows 25 and 26, were necessary. Given that these images were intended for fault mapping and analysis, they needed to be cloud-free and as much as possible to minimize atmospheric distortion. A thorough search was conducted of recent Landsat eight and 9 OLI/TIRS satellite images that met these

criteria, and the image from 2024/08/27 was identified as the most suitable for the study (https://earthexplorer.usgs.gov/). The short-wave infrared (SWIR) bands of Landsat imagery are sensitive to the mineralogical composition of the Earth's surface, making them particularly valuable for lithological classification and detecting variations in rock types. The blue band (visible spectrum) facilitates the further differentiation of materials based on their reflectance characteristics. This combination can highlight differences in rock and soil composition, as well as detect fault zones due to changes in surface materials and topography (Pournamdari et al., 2014). Band combinations of SWIR-2 (7), SWIR-1 (6), and blue (2) are particularly useful for identifying geological formations, lithology features, and faults. A process of fault digitizing was carried out on conventional geological maps and other fault-related data. Nonetheless, the resolution proved to be unsatisfactory. Consequently, we conducted a visual validation of the faults derived from MrVBF and Landsat band combinations. This approach was adopted due to the presence of significant noise in the data extracted from the satellite imagery.

3.2 Spatial improvement analysis

Geological interpretation of specific areas on Earth's surface is based on analyzing geomorphological features depicted in satellite imagery and numerical data, identifying interpretative criteria, and synthesizing results (Theilen-Willige et al., 2016; Canty, 2019; Nixon and Aguado, 2019). Spatial enhancement techniques, such as Sobel contrast filtering, are used to improve clarity and interpretability of geomorphological features in satellite imagery, allowing for more detailed analysis of landforms and their spatial distribution (Enkhbold et al., 2022a; b). The spatial enhancement method was applied to detect tectonic fractures on the surface using a Sobel directional filter on the original satellite imagery (Theilen-Willige et al., 2016). The Sobel function approximates the Sobel edge enhancement operator for satellite images (Equations 1–3).

$$G_{jk} = /G_x/ + /G_y/ \tag{1}$$

$$G_X = F_{j+1,k+1} + 2F_{j+1,k} + F_{j+1,k-1} - \left(F_{j-1,k+1} + 2F_{j-1,k} + F_{j-1,k-1}\right) \tag{2}$$

$$G_Y = F_{j-1,k-1} + 2F_{j,k-1} + F_{j+1,k-1} - \left(F_{j-1,k+1} + 2F_{j,k+1} + F_{j+1,k+1}\right) \tag{3}$$

The Sobel filter is used to detect edges in an image by measuring changes in brightness. It calculates how the brightness changes in two directions: horizontally (Gx) and vertically (Gy). At each pixel, the filter uses two small grids of number sto estimate these changes. This process is called convolution and is done across the entire image, using the pixel's position, labeled as (j, k), in the satellite image (Equation 4).

$$Ymask = \begin{matrix} 1 & 2 & 1 \\ 0 & 0 & 0 \\ -1 & -2 & -1 \end{matrix} \quad Xmask = \begin{matrix} -1 & 0 & 1 \\ -2 & 0 & 2 \\ -1 & 0 & 1 \end{matrix} \tag{4}$$

All edge points in the results are set to zero. We applied horizontal and vertical Sobel filters using the Image Analysis toolbox in ArcMap 10.4. To identify bidirectional line features in satellite images, we generated two filtered images (x- and y-directional), where the highest values indicate line edges, appearing in white. This method modifies the pixel values of the satellite image by incorporating surrounding pixel values.

The Sobel operator was chosen for its balance of robustness and efficiency compared to simpler filters such as Prewitt or Roberts. It is also easier to implement and faster than more complex methods like the Canny edge detector (Theilen-Willige et al., 2016; Nixon and Aguado, 2019). In images processed using the Sobel filter, linear and segmented features associated with tectonic movements are more distinctly highlighted (Vijayarani and Vinupriya, 2013; Aher et al., 2014; Canty, 2019; Theilen-Willige et al., 2016; Nixon and Aguado, 2019).

Landsat TM imagery was primarily used to identify fractures, which were then verified through field observations and the integration of other remote sensing data. The tectonic fractures of the lake depression were mapped using Landsat TM satellite imagery with a 30-m resolution. The data was processed in ENVI 5.3 remote sensing software using the 'Directional Filter' command under the 'Convolution and Morphology' menu. The ENVI 5.3 was selected due to its advanced features, reliability, and user-friendly interface, making it suitable for directional filtering.

3.3 Morphometric analysis

In this study, morphometric analysis is used to quantify the shape, size, and spatial attributes of the lake depressions, providing a foundation for interpreting their geomorphological evolution before applying of specific analytical indices (Jacques et al., 2014; Hassen et al., 2014; Manchar et al., 2022).

Morphometric analysis is also commonly employed in neotectonics studies to identify faulting and land surface structures, thereby emproving the understanding of tectonic processes and landscape evolution (Filosofov, 1967; Pinter and Keller, 1995; Florinsky, 1996; Singh, 2008; Jacques et al., 2014; Hassen et al., 2014; Derikvand and Farahpour, 2020; Ezati et al., 2021; Enkhbold et al., 2022a; b, c; Manchar et al., 2022; Enkhbold et al., 2024a; Taib et al., 2024).

Morphometric analysis reveals the relationships and spatial distributions of various morphometric parameters, showing strong correlations between area, perimeter, and elongation ratio (Singh, 2008). DEM maps have the precision of tectonic geomorphology assessments (Grohmann et al., 2007; Grohmann, 2018) and tectonic characterization (Singh et al., 2012; Whipple and Gasparini, 2014). Morphometric analysis remains a crucial tool in geomorphology, with applications ranging from watershed management to tectonic studies (Ezati et al., 2021). In this study, morphometric indices such as Hypsometric Integral (HI), Mountain front sinuosity (Smf), Basin Shape index (Bs), Relief Slope (RSl), and Relief Energy (RE) were used. Each of these indices provides a unique perspective on the tectonic processes influencing the landscape, allowing for a more comprehensive understanding of fault-related features and the development of lake depressions.

The Hypsometric Integral (HI) is a dimensionless metric used to quantify the distribution of elevation within a drainage basin (Strahler, 1952; Singh, 2008). The index is defined as the area below the hypsometric curve and thus expresses the volume of a basin that

TABLE 1 Basin shape (Bs) index values are used to classify tectonic activity levels (El Hamdouni et al., 2008; Anand and Pradhan, 2019; Das et al., 2022).

Tectonic activity	Bs index	Basin shape
Highly active	≥2.3	Elongated
Moderately active	1.2 to 2.3	Less elongated or oval
Less or inactive	≤1.2	Circular

has not been eroded (Pinter and Keller, 1995; Hassen et al., 2014). A lake depression with a high HI may indicate significant tectonic activity shaping the basin, while a low HI could suggest more erosion and a less tectonically active basin. Mathematically, it is expressed as (Equation 5):

$$HI\,(\%) = (Emean - Emin)/(Emax - Emin) \quad (5)$$

where E_{mean} is the mean elevation, E_{min} is the minimum elevation, and E_{max} is the maximum elevation of the depression. A high HI value (>0.5) indicates a youthful stage of land surface evolution, while a low HI value (<0.4) suggests a mature or old stage with significant erosion (Strahler, 1952; Strahler, 1964; Pinter and Keller, 1995; Hassen et al., 2014; Farhan et al., 2016a; Maliqi et al., 2023).

The Mountain Front Sinuosity (Smf) is a morphometric index employed to evaluate the degree of tectonic activity along mountain fronts (Keller and Pinter, 2002; Silva et al., 2003). It is calculated as follows (Equation 6):

$$Smf = L_{mf}/L_s \quad (6)$$

where Lmf is the total length of the mountain front along the contact between the mountain and the adjacent depression, and Ls is the straight-line length of the mountain front (Bull and McFadden, 1980). A Smf value below 1.4 indicates active tectonics, with uplift prevailing over erosion, tectonically stable or eroded front (Keller and Pinter, 2002). In contrast, Smf values above 1.5 suggest less tectonically active or more erosional fronts, often characterized by irregular or sinuous shapes due to erosional processes (Bull and McFadden, 1980).

The Basin Shape index (Bs) in tectonically active mountain ranges is generally more elongated but tends to evolve into a more circular form over time (El Hamdouni et al., 2008). In the mountainous region, the presence of narrow, elongated basins along the Main Frontal Thrust and Main Boundary Thrust indicates recent tectonic uplift and ongoing fault activity (Anand and Pradhan, 2019; Taib et al., 2024). It is defined by the following ratio (Equation 7):

$$Bs = Bl/Bw \quad (7)$$

Here, *Bl* represents the measured length from the headwater to the mouth of the basin, while *Bw* denotes the width measured at the widest point of the basin (Ramírez-Herrera, 1998). A higher Bs value indicates a more elongated basin, while a lower value suggests a more circular or compact basin (Table 1).

Relief Slope analysis (RSl) is an effective tool for identifying fault structures within lake depressions by evaluating two primary indicators: steep side slopes, which suggest abrupt changes in surface gradient, and relative elevation differences, which point to vertical displacement along fault lines. These geomorphic signals are often corroborated by characteristic patterns in hypsometric curves (Jordan, 2003; Farhan et al., 2016b; Enkhbold et al., 2022a; Enkhbold et al., 2022b). Previous studies have demonstrated the utility of RSl analysis in identifying fault structures within lake depressions (Onorato et al., 2017; Korzhenkov et al., 2019). In this study, RSl values were derived from satellite-based digital elevation models (DEMs) and visualized as spatial maps to detect abrupt changes in slope. The resulting spatial patterns highlight zones of steep gradients and relative elevation discontinuities, which often correspond to inferred fault traces (Gürbüz and Gürer, 2008). These interpretations are further substantiated by hypsometric curve analysis, which quantitatively characterizes the elevation distribution within the basin (Hooper et al., 2003; Farhan and Anaba, 2016). The likelihood of fault presence can be assessed based on surface slope characteristics within the lake depression. Specifically, RSl values indicate different probabilities of faulting: RSl <5° is low probability of faulting, 5°<RSl< 10° is possible fault presence, and RSl >10° is the high probability of a fault (Bucknam and Anderson, 1979; Hooper et al., 2003; Ganas et al., 2005; Gürbüz and Gürer, 2008; Onorato et al., 2017; Korzhenkov et al., 2019; Enkhbold et al., 2022a; Enkhbold et al., 2022b).

A straight-line appearance along the sloping surface suggests alignment with a fault. The greater the visible length of this linear feature, the higher the likelihood of fault presence (Hooper et al., 2003; Onorato et al., 2017; Korzhenkov et al., 2019; Enkhbold et al., 2022a, b). For this study, RSl values were calculated using spatial resolution imagery from DEM (30 m).

Morphometric analysis based on Relief Energy (RE) indicators provides another method for fault identification on land surfaces (Kot, 2018; Enkhbold et al., 2022b). RE represents the difference in relative height across the surface (Di Crescenzo and Santo, 2005). Faults can be detected by abrupt variations in RE values (Di Crescenzo and Santo, 2005; Kot, 2018; Enkhbold et al., 2022b). The RE value is calculated using the following (Equation 8):

$$RE = H_{max} - H_{min} \quad (8)$$

Where RE is the Relief Energy (m), Hmax is the maximum surface height (m), and Hmin is the minimum surface height (m). Using a hypsometric curve, the upper, middle, and lower dimensions of relative surface height can be determined. In mountainous terrain, RE values up to 50 m indicate a low probability of a fault, values between 51 and 150 m indicate a medium probability, values between 151 and 500 m indicate a high probability, and values exceeding 500 m indicate a very high probability of a fault (Hooper et al., 2003; Di Crescenzo and Santo, 2005; Kot, 2018; Enkhbold et al., 2022a, b).

3.4 Analysis of geomorphological criteria

This criterion indicator relates to the determination of the origins of lake depressions by systematically identifying

TABLE 2 Suitability matrix of geomorphological criteria (Adapted from Enkhbold et al., 2024a).

N°	Compliance ratio	Conformity suitability	Percent, %
1	0 > 3	Not compliance	0–30
2	3 > 4	Less compliance	31–40
3	5 > 7	Compliance	51–70
4	7 > 9	Good compliance	71–90
5	9 < 10	Excellent compliance	91–100

and hierarchically ranking the factors contributing to their formation. As noted by Cohen (2003), the genesis of lake basins can be elucidated by assessing the relative contributions of tectonic processes, glacial dynamics, climatic conditions, and geomorphological evolution, thereby providing a comprehensive understanding of the mechanisms shaping lake depression morphology (Enkhbold et al., 2024a). To achieve this, the primary and secondary factors affecting lake depressions are analyzed based on their geomorphological characteristics (Hughes, 2010; Church, 2013). Although the morphological features shaped by these factors are challenging to quantify, researchers can evaluate the genetic characteristics of landforms within a defined spatial framework using specific assessment criteria (Bishop et al., 2012; Enkhbold et al., 2021; Enkhbold et al., 2022a; Enkhbold et al., 2022b; Enkhbold et al., 2022c; Enkhbold et al., 2022d).

The ten criteria for classifying lake depressions were developed based on geomorphological analysis of field and map materials. Determining the origin of these depressions involves two steps: first, analyzing geomorphological patterns, field measurements, and geological research documents, and second, using mapping methods to identify and confirm the factors influencing their formation. The typology is assessed through a suitability matrix of geomorphological criteria (Table 2).

In this study, tectonic geomorphological criteria were developed to facilitate a comparative analysis of the origin and morphological characteristics of the Achit, Uureg, and Tolbo lake depressions (see Table 5 for criteria).

4 Results

4.1 Satellite map interpretation

In the MAM region, significant faults trending northwest to southeast are still causing block to experience uplift and subsidence (Cunningham et al., 2003; Howard et al., 2003; Cunningham, 2005; Khukhuudei et al., 2024).

The Achit Lake depression covers an area of 2235.51 km^2, the Uureg Lake depression spans 768.13 km^2, and the Tolbo Lake depression, the smallest of the three, has an area of 345.79 km^2.

The satellite-based structural interpretation delineates the digitized mapping of primary and subsidiary faults (Tamani et al., 2019; Chibani et al., 2022), derived through MrVBF analysis. This interpretation integrates a band combination of SWIR-2, SWIR-1, and blue wavelengths to enhance fault structural contrasts, complemented by a Landsat 9 OLI/TIRS image (30 m resolution) processed with spatial enhancement techniques to accentuate fault patterns. Collectively, these datasets provide a comprehensive structural framework that is critical for the tectonic geomorphological analysis of the study area (Figure 3).

The tectonic influence on the lake depressions was more distinctly revealed through the analysis of image overlaps discrepancies, fault mapping, and the construction of cross-sectional profiles. These steps enabled a detailed understanding of how tectonic movements shape the MAM distribution of the lake depressions.

The interpretation of satellite imagery highlights the fundamental tectonic features of the MAM, with a particular focus on the relationship between fault structures and the formation of lake depressions. The structural interpretation, based on satellite imagery, offers a comprehensive and digitized map of both primary and secondary fault lines (Tamani et al., 2019; Taib et al., 2024), delineated through MrVBF analysis (Figure 3A). This approach incorporates a combination of SWIR-2, SWIR-1, and blue wavelengths, effectively accentuating lithological and structural contrasts. Additionally, a Landsat 9 OLI/TIRS image (with a spatial resolution of 30 m) was processed using advanced spatial enhancement techniques to improve the visibility of fault patterns (Figure 3B). The results are analyzed within the framework of the faulting system that extends from the northwest to the southeast of the MAM, correlating tectonic processes with the formation of these distinctive features. This study provides critical insight into the structural controls influencing lake depressions, thereby contributing to a deeper understanding of the region's tectonic evolution. The fault lines identified by satellite imagery were highlighted and marked using a spatial enhancement method applied to the linear spectrum on the satellite image (Figure 3C).

The tectonic geomorphological features of the Tolbo, Achit, and Uureg Lake depressions were systematically analyzed and characterized through the validation of satellite imagery, a method that facilitated detailed observation and interpretation of the landscape. High-resolution satellite images were utilized to identify and map key features such as fault lines and other tectonically influenced formations. The satellite-based approach enabled the identification of fault patterns and their spatial relationships, offering key insights into the tectonic evolution of the Tolbo, Achit, and Uureg lake depressions. This method provided a concise framework for understanding their geomorphological development.

4.2 Morphometric analysis interpretation

Morphometric analysis based on satellite imagery is essential for accurately defining the size, shape, structure, and geometric characteristics of lake depressions (Jordan, 2003; Hooper et al., 2003; Jacques et al., 2014; Onorato et al., 2017; Enkhbold et al., 2022a, b, c). First, Mountain front sinuosity (Smf) and Hypsometric Integral (HI) were calculated in the study area (Figure 4).

The HI (%) analysis of the Uureg Lake depression revealed an HI (%) value of 0.67 between elevations of 2000–2500 m.a.s.l along the

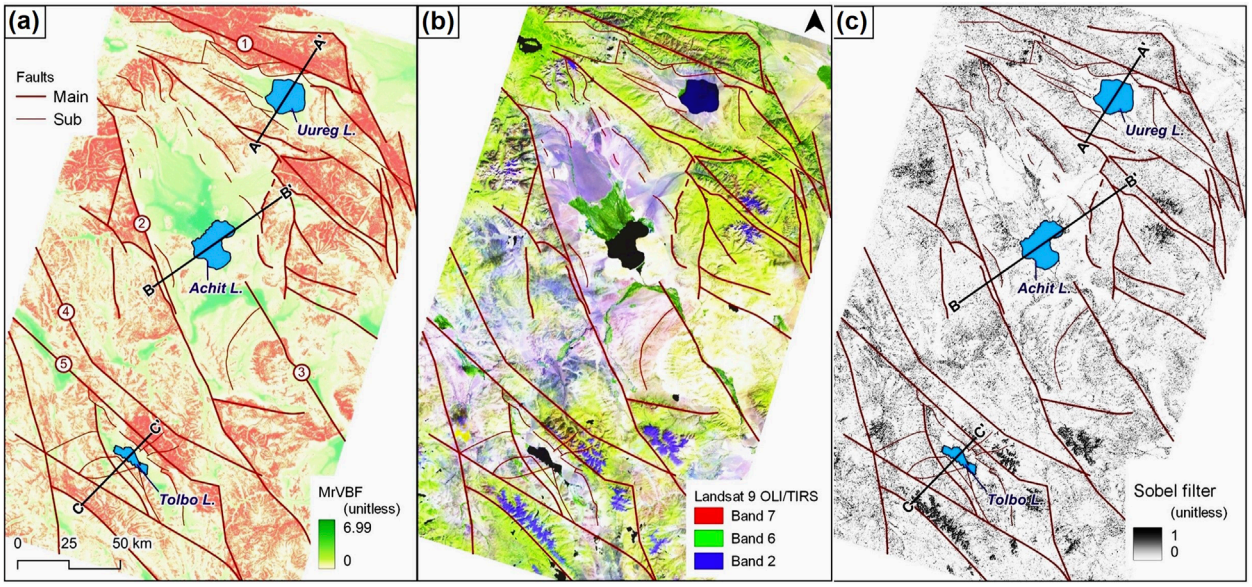

FIGURE 3
(a) Digitized main and sub-faults based on the MrVBF, **(b)** clarification on the band combination of SWIR-2, SWIR-1, and blue, **(c)** Landsat 9 OLI/TISR Satellite (30-m) image processed by spatial improvement method, shown faults.

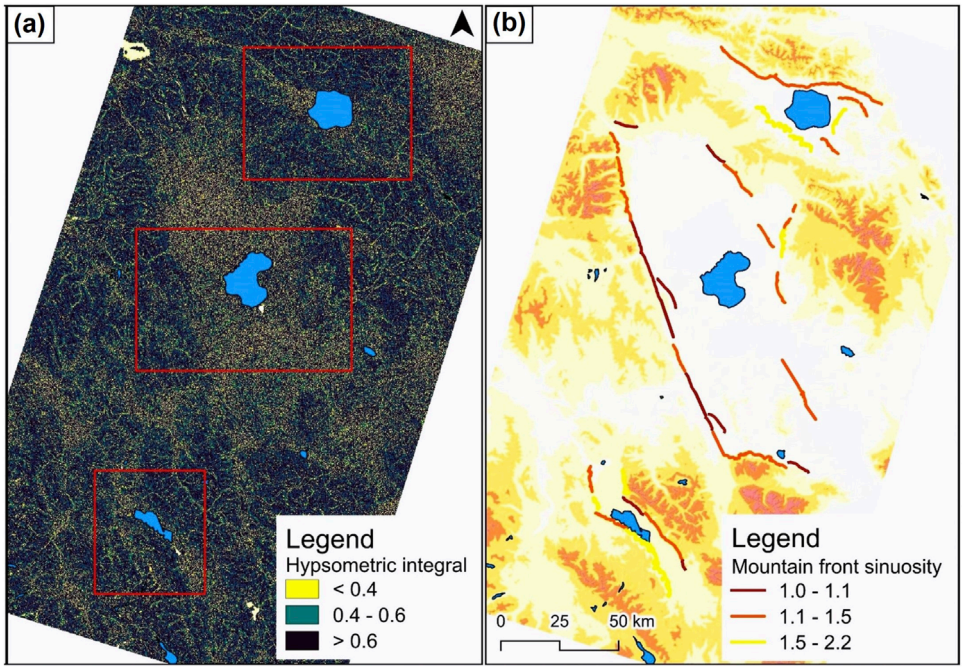

FIGURE 4
(a) Hypsometric Integral (HI) map of the study area, **(b)** Mountain Front Sinuosity (Smf).

Tsagaan Shuvuut fault and 0.56 between 1,600 and 2000 m.a.s.l along the Bayram fault. In the Achit Lake depression, the HI (%) value was 0.57 between 1900 and 2400 m.a.s.l along the Khovd fault and 0.51 between 2000 and 2300 m.a.s.l along the Khundlun Uul fault. The HI (%) analysis of the Tolbo Lake depression showed a value of 0.77 between 2100 and 2500 m.a.s.l along the Tolbo Nuur fault, while the fault on the southern side of Tolbo Lake had an HI (%) value of 0.76 between 2200 and 2600 m.a.s.l above sea level (Figure 4a).

The morphometric Smf analysis of the Uureg Lake depression indicated index values along the Tsagaan Shuvuut fault ranging from 1.1 to 1.5. The whereas the Bayram fault exhibited index values between 1.5 and 2.2. In the western portion of the Achit Lake

TABLE 3 Basin shape index (Bs) of three lakes depression.

Depression	Length	Width	Bs index	Tectonic activity
Uureg lake	69.3	41.9	1.65	Moderate active
Achit lake	161.1	88.8	1.81	Moderate active
Tolbo lake	55.9	18.3	3.05	Highly active

depression, the Khovd fault showed index values between 1.0 and 1.1, while in the eastern part of the depression, the Smf index values along the Khundlun Uul fault ranged from 1.1 to 1.5. Along the Tolbo Nuur fault in the northern part of the Tolbo Lake depression, the Smf index values ranged from 1.0 to 1.1 and from 1.1 to 1.5, indicating active tectonics. In the southern part of the depression, the Smf index values ranged from 1.1 to 1.5 and 1.5 to 2.2, signifying active tectonics (Figure 4b).

Morphometric Basin shape index (Bs) of three different lake depressions was calculated (Table 3).

The Bs index value ranged from 1.65 to 1.81 in the Uureg and Achit lake depressions, indicating moderate activity, and was 3.05 in the Tolbo lake depression, indicating high activity.

Hypsometric RSl analysis examines the distribution of elevations within a specific area, such as a lake basin. The results are typically presented as hypsometric curves, which help interpret the geomorphic development stage and the tectonic history of the landscape (Hooper et al., 2003; Farhan and Anaba, 2016). The RSL values within the hypsometric curve were calculated using hypsometric cross-sectional profiles constructed along the studied lake basins. These profiles facilitated the identification of fault patterns and the assessment of their geomorphic influence. Based on the distribution and orientation of the fault systems, a conceptual basin model was developed and refined (Figure 5).

In the northern part of the Uureg Lake depression, morphometric RSl analysis revealed steep slopes ranging from 38° to 42° along the Tsagaan Shuvuut thrust fault at elevations between 2000 and 2500 m, whereas the Bayram fault in the southern sector showed gentler slopes of 21°–24°. In the western margin of the Achit Lake depression, slope angles of 41°–44° were identified along the Khovd strike-slip fault at elevations of 1900–2400 m, while the eastern Khundlun Uul fault exhibited lower slopes of 19°–23°. Similarly, in the northern part of the Tolbo Lake depression, the tilted thrust fault along Tolbo Nuur displayed slopes of 41°–47% at 2100–2500 m, contrasting with gentler slopes of 17°–19° in the southern segment. The variation in surface slope angles along bounding faults of the lake depressions suggests a high likelihood of recent or ongoing fault activity.

Exposures of Oligocene to recent strata within upturned belts along the MAM provide evidence that Cenozoic tectonic rejuvenation began during the Oligocene and has continued to the present (Howard et al., 2003; Cunningham, 2005; Khukhuudei et al., 2024). The MAM is characterized by various basin types, including half-ramp, ramp, and foreland basins, as well as pull-apart, strike-slip, open thrust, and remnant low basins (Cunningham, 2005). These basins are shaped by diverse tectonic processes, such as active thrusting, strike-slip faulting, and sediment accumulation in tectonically stable areas.

The northern margin of the Uureg Lake depression is controlled by a thrust fault associated with the Tsagaanshuvuut Fault (Emanov et al., 2012; Khukhuudei et al., 2024), indicating that the depression corresponds to an ramp basin model. In the case of the Achit Lake depression, its western boundary is the Khovd fault (Davaasambuu et al., 2023; Ha et al., 2023), while the eastern margin is bounded by the Khundlun Mountain fault, which has resulted in the formation of a remnant low basin. This structural configuration is consistent with a ramp basin model. Similarly, the northern portion of the Tolbo Lake depression is controlled by the Tolbo Nuur fault (Baljinnyam, 1993), suggesting that the depression conforms to a half-ramp basin model.

This type of depression type is typically observed in regions where tectonic and erosional forces have shaped the landscape, resulting in a gently sloping surface that promotes the accumulation of water or sediments. Studying such a basin type is essential for understanding the dynamics of hydrology, sediment transport, and overall landscape evolution in the region.

Morphometric RE analysis was conducted to determine the highest, lowest, and average surface elevations of the three lakes in the study area. The comparative morphometric characteristics of the lake depressions in the study area were calculated using 'Landsat TM' satellite imagery from the 'Global Visualization Viewer' (GloVis) (Table 4).

Based on the morphometric parameters of the three studied lake depressions, Reanalysis was conducted. The results revealed that the Achit Lake basin exhibited a high likelihood of tectonic activity, whereas the basins of Uureg and Tolbo Lakes demonstrated a very high likelihood of tectonic influence.

By comparing the morphometric parameters across the Achit, Uureg, and Tolbo lake depressions, we were able to identify their spatial patterns and provide a comprehensive interpretation of the morphometric analysis. This analysis offers valuable insights into the tectonic processes that have shaped these features. The spatial distribution and morphological characteristics of these lake depressions reflect ongoing tectonic activity in the MAM region, where faulting, uplift, and subsidence have significantly influenced their development. Each depression displays distinct geomorphological features, underscoring the interaction between tectonic forces and sedimentary processes.

4.3 Geomorphological criteria interpretation

Interpretating geomorphological criteria involves assessing landforms, geological structures, and surface processes to understand the dynamics of a given region (Green and White, 2019; Smith, 2020). This interpretation relies on analyzing landforms such as mountains, valleys, and plains, as well as the processes shaping them, including erosion, sediment transport, and tectonic activity (Hughes, 2010; Bishop et al., 2012; Church, 2013; Enkhbold et al., 2021; Enkhbold et al., 2024a). These criteria aim to detect tectonic activity and characterize the geomorphological features surrounding a lake. Specifically, tectonic shifts, earthquakes, and volcanic processes play a crucial role in influencing the

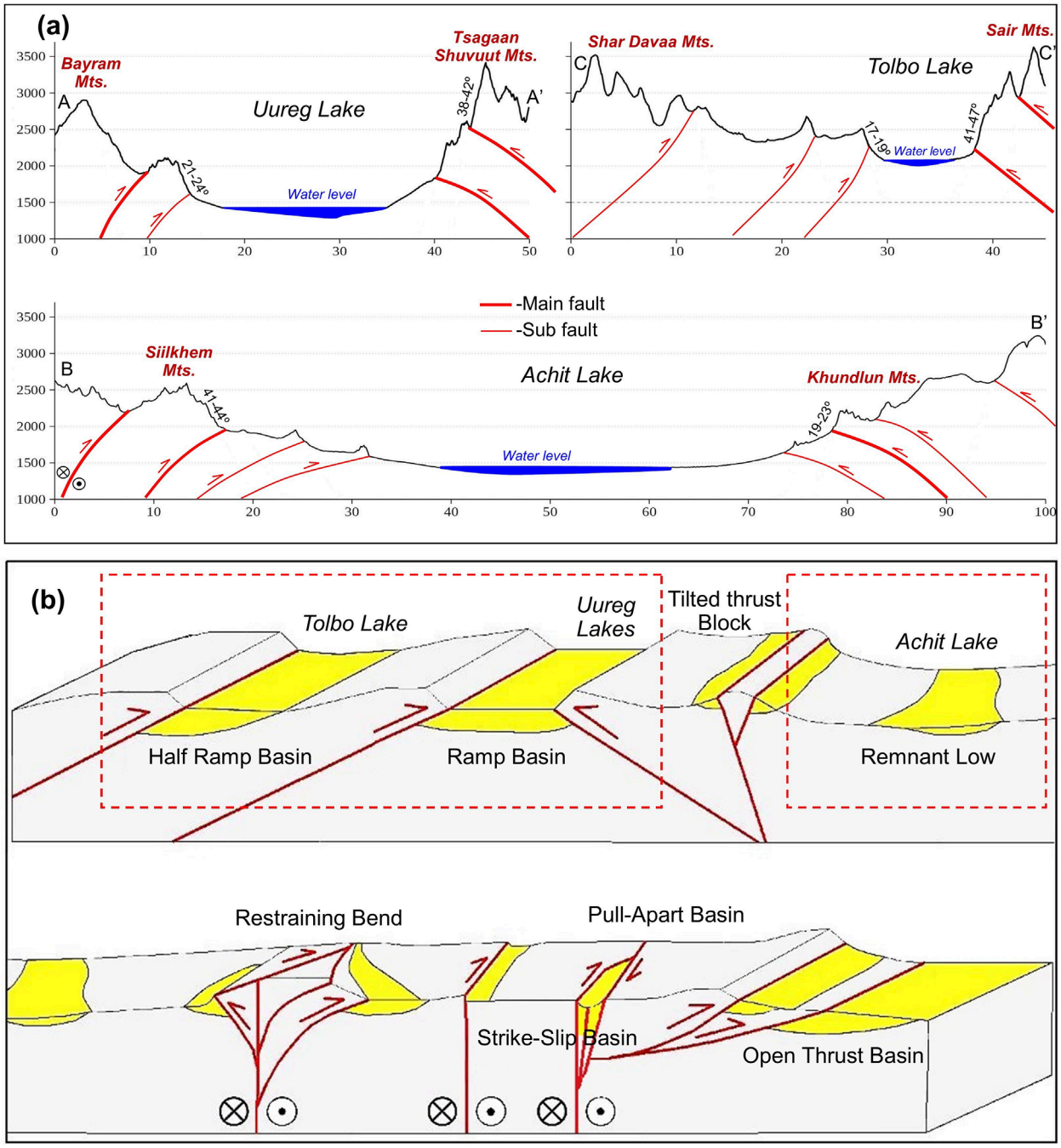

FIGURE 5
(a) Hypsometric cross-section illustrating the faults and surface slopes that contributed to the formation of the lake depression. **(b)** Genetic model depicting the types of mountain ranges and basins in the MAM (adapted from Cunningham, 2005; Khukhuudei et al., 2024).

formation, topography, elevation, and water levels of the lake and its surrounding landscape (Church, 2013; Enkhbold et al., 2021). In this study, ten criteria were evaluated to clarify the origin and tectonic geomorphological influence of the lake depression (Table 5).

Based on tectonic geomorphological criteria for defining lake depressions, the Achit Lake depression meets 6, the Uureg Lake depression 9, and the Tolbo Lake depression eight criteria consistent with a tectonic origin. The tectonic influence on the depressions of the lakes examined in this study shows a strong correlation, with compliance ranging from 60 to 90 percent. This indicates a high degree of consistency and a significant contribution to the formation of these depressions. It suggests that tectonic processes play a crucial role in shaping the lake basins, with their influence accounting for a substantial portion of the observed geomorphological features.

Upon synthesizing the study results, it becomes clear that the spatial distribution of tectonic faults and surface features observed in the MAM lake depressions, along with the direction of tectonic movement and transitional patterns across Mongolia, suggest that

TABLE 4 Morphometric parameter of Lake depressions.

N°	Lake name	Length (km)	Width (km)	Area (km^2)	Elevation, m.a.s.l (m)			RE (m)	Probability
					Low	Medium	High		
1	Uureg	161.1	88.8	768.13	1,383	1,666	2406	1,023	Very high
2	Achit	69.3	41.9	2235.51	1,429	1,549	1827	398	High
3	Tolbo	55.9	18.3	345.79	2062	2237	2663	601	Very high

TABLE 5 Analysis of geomorphological criteria indicators.

N°	Criteria Indicators (Compatibility +, Incompatibility –)	Achit	Uureg	Tolbo
1	Whether a tectonic fault is present around the lake depression	+	+	+
2	Whether the drainage depression of the lake is 2–4 times larger than the lake's surface area	+	+	+
3	Whether the lake depression is located at an altitude of 500 m or higher	+	+	+
4	Whether the difference in elevation between the surrounding mountains and the lake depression exceeds 600 m	–	+	+
5	Whether volcanic rocks are present in the area around the lake depression	–	+	–
6	Whether an island composed of original bedrock exists in the lake	–	–	+
7	Whether the lake has steep shores and an uneven lakebed morphology	–	+	+
8	Whether the surrounding depression is constricted or elongated, and whether the lake's surface area is irregularly shaped	+	+	+
9	Whether the shoreline is heavily indented, and whether there are significant distortions in the bathymetric data	+	+	–
10	Whether the lake water is fresh, deep, and has a large volume relative to its size	+	+	+
	Number of Compliances	6	9	8

the origins of these three lake depressions likely developed under similar geological conditions. The faults within the study area are depicted in the images below (Figure 6).

An interpretation of geomorphological criteria was conducted on the lake basins. This involved a comprehensive analysis based on specific criteria, aimed at identifying key features and their corresponding geomorphological forms.

The interpretation of these tectonic geomorphological criteria reveled that, the MAM lake depressions are classified as tectonic depressions. Satellite imagery, morphometric analysis, and geomorphological criteria revealed prominent fault structures that define the boundaries of these depressions, confirming the role of extensional tectonic forces in their formation. These forces have caused the crust to fracture and sink between parallel fault lines, resulting in the distinct basin-like structures observed in the region. The northern MAM are in the transpressional stress field, the basins should be consistent with it and all intermontane basis are either half ramp or ramp basins.

The Uureg Lake depression is bordered by a tectonic fault system. The Tsagaan Shuvuut Fault trends parallel to the northern boundary of the lake basin in a northwest-southeast direction, while the Bayram Fault runs parallel to the southern boundary of the lake, also following a northwest-southeast orientation. The northern boundary of the lake depression is defined by the Tsagaan Shuvuut fault, while the western and southwestern boundaries are delineated by the Western Bayram fault. The central portion of the depression is shaped by faults linked to Uureg Lake. Notably, a significant earthquake with a magnitude of 7.0 occurred along the Tsagaan Shuvuut fault in 1970, and the region remains an area of high seismic activity (Emanov et al., 2012). The drainage basin of the lake is 2–4 times larger than the surface area of the lake itself. The lake depression is located at an altitude of 500 m or higher, with an elevation difference of more than 600 m between the surrounding mountains and the lake depression. Volcanic rocks are present in the area surrounding the lake depression. The lake features steep shores and an uneven lakebed morphology. The surrounding depression is either constricted or elongated. The lake's surface area is irregularly shaped, and its shoreline is heavily indented. Significant distortions may be present in the bathymetric data. The lake water is deep and possesses a large volume relative to its size.

The dominant fault structures within the Uureg Lake Depression were further verified through the hypsometric cross-sections

FIGURE 6
Interpretation of field photographs. **(a)** View of the Tsagaan Shuvuut fault, located north of the Urekh Lake depression, **(b)** View of the Khovd fault, situated west of the Achit Lake depression, **(c)** View of to the north of Tolbo Nuur fault (Photos taken by Altanbold Enkhbold, Alexander Perin, Alexander Strekhletov, B. Batzorig, and B. Zolbadral).

analysis. Specifically, the Tsagaan Shuvuut Fault has played a significant role in shaping the morphology of the depression, which is enclosed within a closed basin and surrounded by medium to high mountain ranges. The development of pediments along the mountain ranges indicates a high degree of relief energy difference within the depression.

At an elevation of 42 m above the current water level of Uureg Lake, five to six distinct gravel terraces have been identified (Tserensodnom, 1971). Although this study does not provide direct chronological data on sedimentary deposits or gravel terraces from Uureg Lake itself, regional chronological records from adjacent basins - such as Khyargas and Orog Lakes—offer valuable insights into shared tectonic and climatic influences. Incorporating these data enhances the interpretation of terrace formation and broader landscape evolution in a regional geomorphic and temporal framework. Recent studies have established chronological constraints on gravel terraces and paleo-shoreline features around Khyargas and Orog Lakes, aiming to reconstruct past hydrological and tectonic regimes (Nottebaum et al., 2022; Zhang J. et al., 2022; Wolf et al., 2025; Rahimzadeh et al., 2025). Optically stimulated luminescence (OSL) dating by Nottebaum et al. (2022) and Zhang S. et al. (2022) indicates the existence of a paleolake at Orog Lake, with water levels reaching 56 m above the present lake level approximately 124.2 ± 6.8 ka ago. At that time, the lake's volume was estimated at 24.5 km^3 - approximately 153 times greater than its modern capacity. Subsequent highstands occurred at 23 m above the current level around 11.1 ± 1.0 ka, and between 14 and 20 m around 6.7 ± 0.8 ka. Similarly, OSL dating by Wolf et al. (2025) and Rahimzadeh et al. (2025) on shoreline terraces at Lake Khyargas revealed that a terrace located 129 m above the present lake level formed between 104.7 ± 14.4 ka and 88.8 ± 12.7 ka. An additional terrace at 118 m was dated to approximately 14 ka, while terraces ranging from 7 to 15 m were formed during the late Holocene. Taken together, the paleo shoreline terraces of Lakes Orog and Khyargas reflect significant lake-level fluctuations spanning from the Late Pleistocene through the early, middle, and late Holocene (Lehmkuhl and Lang, 2001; Lehmkuhl et al., 2018b; Nottebaum et al., 2022; Zhang J. et al., 2022; Wolf et al., 2025; Rahimzadeh et al., 2025). These findings support the interpretation that the gravel terraces at Uureg Lake likely represent analogous coastal features formed during the same periods of climatic and hydrological change. It has been established that the primary source of these water

inputs during the Late Quaternary was meltwater originating from the Altai and Khangai Mountains (Lehmkuhl and Lang, 2001; Lehmkuhl, 2016; Lehmkuhl et al., 2018a; Lehmkuhl et al., 2018b; Klinge et al., 2021; Wolf et al., 2025).

The Achit Lake depression is enclosed by a tectonic fault. Analysis of the graben structures within the study area reveals several parallel fault lines along the western and eastern boundaries of the Achit Lake Depression. The drainage basin of the lake is approximately 2–4 times larger than the lake's surface area. The depression is situated at an altitude of 500 m or higher. The surrounding depression exhibits constriction or elongation, and the lake's surface area is irregularly shaped. The shoreline exhibits considerable indentation, and the bathymetric data show significant distortions. Additionally, the lake water is fresh, deep, and contains a large volume relative to its size.

Upon interpreting the surface features of the Achit Lake Depression and considering the dominant tectonic movement directions and transitional patterns in Mongolia, it is evident that the primary morphological structure of this depression aligns with a tectonic-origin graben formation. The depression is bordered by parallel tectonic fault lines, forming a downthrown graben structure.

Cross-sectional analysis of the Achit Lake Depression indicates that the western side, bounded by the Siilkhem Mountain range and the Khovd fault, exerts a significant influence on the depression's morphology. Along the Khovd fault, a large pediment has developed in the western portion of the depression. In terms of relief, the western section is marked by steep mountain ranges, whereas the eastern side is characterized by relatively gentle, sloping surfaces. The depression is enclosed by parallel fault lines, and the notable down warping of the depression suggests the formation of an extensive drainage area, which implies a high-water storage capacity.

Studies have reported significant fluctuations in water levels within the lake depression. Particularly during the early Holocene, the lake level was 50–60 m higher than it is currently, resulting in the formation of lake terraces along the northeastern shore (Agatova and Nepop, 2019; Oyunchimeg and Narantsetseg, 2020). These fluctuations have led to rapid increases and decreases in water levels, causing noticeable change in the surrounding surface. Chronological analysis of the depression's sediments has dated the Holocene sediments to approximately 11,500 ± 150 years (Tserensodnom, 2000). However, Sun et al. (2013) conducted a detailed analysis of a sediment sample from 200 cm below the lakebed, revealing a chronology of approximately 19,969 ± 110 years. While this chronology is only partially linked to the primary formation of the lake depression, it is crucial for understanding the sedimentation processes, tectonic dynamics, and the broader chronological context of the lake's history.

The Tolbo Lake depression is bounded by a tectonic fault, with the Tolbo Nuur fault located to the north of the depression. Surface features observed in the Tolbo Lake Depression, when analyzed and interpreted, indicate that the primary structure of the depression is of tectonic origin. The drainage basin of the lake is approximately 2–4 times larger than the lake's surface area. The depression is situated at an altitude of 500 m or higher, with an elevation difference exceeding 600 m between the surrounding mountains and the lake basin. The lake exhibits steep shores and an uneven lakebed morphology. The surrounding depression is characterized by constriction and elongation, while the lake's surface area has an irregular shape. Furthermore, the lake water is fresh, deep, and holds a large volume relative to its size.

The depression is bordered to the north and south by tectonic faults, and it is evident that the Tolbo Lake fault has exerted a significant influence on its morphology. The depression is enclosed by a closed depression, surrounded by medium to high mountains that form a playa-like structure. The development of pediments along the mountain ranges indicates a considerable relief energy difference within the depression. Hydrological and sedimentological studies of Lake Tolbo reveal significant fluctuations in water levels within the lake depression.

Zhang S. et al. (2022) study reconstructs aeolian activity in western Mongolia over the past ~14 ka using sediment grain size data from Tolbo Lake, revealing that intensified late Holocene activity was driven by stronger winds resulting from increased spring insolation and mountain snow, while weaker activity during the middle Holocene correlated with warming in northern latitudes, increased humidity, and limited dust contribution to Greenland. Additionally, Li et al. (2025) studied and reconstructed the water level fluctuations of Tolbo Lake in the Altai Mountains over the past 13.7 kyr using sedimentary cladoceran fossils, showing that the Holocene rise in lake levels was driven by intensified westerly precipitation.

5 Discussion

5.1 Geomorphological features and tectonic influence of the lake basins in the MAM

The present distribution and size of lakes in the mountainous regions of Central Asia, particularly in the MAM, have undergone significant changes compared to the past, as documented by multiple studies (Tserensodnom, 2000; Grunert et al., 2000; Sun et al., 2013; Lehmkuhl, 2016; Agatova and Nepop, 2019; Oyunchimeg and Narantsetseg, 2020; Klinge et al., 2021; Enkhbold et al., 2022d; Zhang J et al., 2022; Hu et al., 2024; Lehmkuhl et al., 2024; Enkhbold et al., 2025a; Li et al., 2025).

Lakes in the MAM typically occupy tectonic depressions formed during the Quaternary due to ongoing tectonic movements related to the India-Asia collision and associated transpressional regimes (Molnar and Tapponnier, 1975; Tapponnier and Molnar, 1979; Nissen et al., 2009ab; Cunningham, 2005; Ha et al., 2023; Ramel et al., 2025). These depressions are controlled by fault systems at mountain-depression boundaries, where mountain blocks experience uplift while adjacent basins subside, creating accommodation space for lake formation (Enkhbold et al., 2024a; Enkhbold et al., 2025b).

Glaciation has further modified the morphology of these depressions, with glaciers sculpting the landscape and leaving behind overdeepened basins and lacustrine terraces (Tserensodnom, 2000; Grunert et al., 2000; Lehmkuhl, 2016; Lehmkuhl et al., 2018a, b; Walther et al., 2024). Thus, the current lake basins represent the integrated effects of tectonic subsidence, glacial erosion, sedimentation, and climate-driven hydrological changes (Figure 7).

Fault-controlled uplift and subsidence create accommodation space for lake formation. Glacial erosion and deposition further

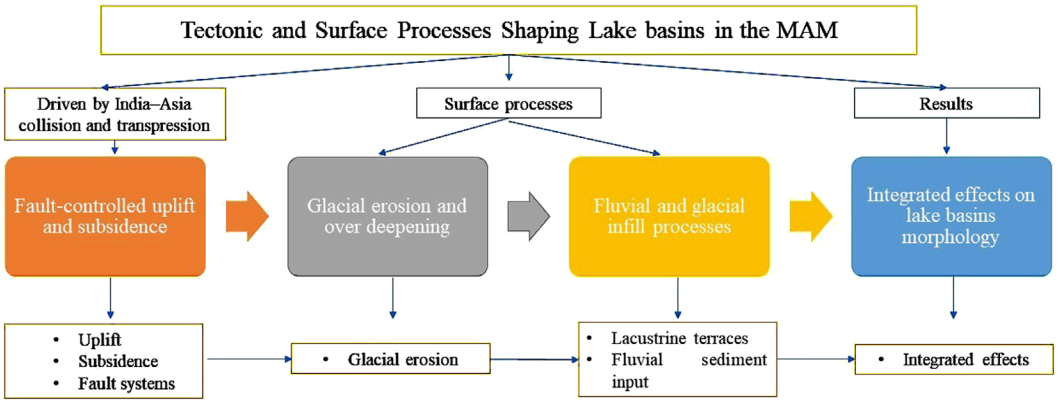

FIGURE 7
Conceptual diagram illustrating the tectonic and surface processes shaping lake basins in the MAM.

modify basin morphology, while fluvial sediment input influences basin infill. The interplay of these endogenic and exogenic factors determines the present-day lake basin features.

While tectonic processes dominate basin formation, exogenic factors such as sediment supply from rivers and weathering contribute significantly to the infill and morphological evolution of these depressions. Fluvial sediments transported from elevated catchments accumulate within tectonically subsiding basins (Agatova and Nepop, 2019; Lehmkuhl et al., 2018a; Lehmkuhl et al., 2018b; Oyunchimeg and Narantsetseg, 2020), modifying lake basin morphology over time (Lehmkuhl, 2016).

The geomorphological characteristics of lake depressions in the MAM are therefore a product of complex interactions between endogenic tectonic activity and exogenic surface processes. This interplay has resulted in distinctive morphological features that allow differentiation of primary tectonic controls from secondary sedimentary modifications (Enkhbold et al., 2022d).

Understanding these relationships is critical for reconstructing the tectonic evolution of the region and assessing landscape development. Future research integrating tectonic geomorphology, sedimentology, and paleoecological data will provide a more comprehensive view of the formation and evolution of these lake basins. A more detailed investigation into the interaction between tectonics and lake depressions is essential for understanding regional tectonic development and the evolution of lake depression morphology. In the future, combining tectonic research with geomorphology, paleoecology, and detailed sedimentary studies will provide a more comprehensive understanding of the historical changes in the lake depressions of the MAM tectonic region.

5.2 Tectonic-driven lake basins in the altai mountains: a geomorphological perspective

The Altai Mountains in Mongolia represent one of the most tectonically dynamic and geomorphologically intriguing regions in Central Asia (Bayasgalan et al., 1999a; Khukhuudei et al., 2024; Enkhbold et al., 2024c). The landscape is distinguished by diverse landforms, including high mountain ridges, deep valleys, and numerous lake depressions, all of which provide valuable insights into the tectonic processes that have shaped the region. A detailed tectonic geomorphological study of these lake depressions reveals the intricate relationship between geological activity and surface processes.

The Altai Mountains are a product of complex tectonic interactions, primarily associated with the collision between the Eurasian and Indian plates (Molnar and Tapponnier, 1975; Molnar and Tapponnier, 1975; Kusky et al., 2016). This region has been shaped by a combination of compression, uplift, and faulting, which has resulted in the creation of significant mountain ranges and basins (Cunningham et al., 1996). These basins, many of which are now filled with lakes, serve as important geological indicators of past and present tectonic activity (Cunningham, 2005).

The fault systems of the MAM play a critical role in shaping the geomorphological characteristics of the region, being directly linked to the formation of lake depressions (Enkhbold et al., 2024c). These faults influence the direction of water flow and sediment accumulation, leading to the formation of lakes along fault lines or the creation of tectonic depressions due to faulting. The activity of these faults alters the landscape, creating conditions favorable for water accumulation, which is essential for the formation and development of lake depressions. The lake depressions in the study area are depressions surrounded by major active high mountains and less active high mountains, situated between transpressional mountain ranges (Figure 8).

The inset box illustrates the major mountain belts in the MAM. The Great Lakes Basin is characterized by isolated mountain ranges bordered by Cenozoic thrust and oblique-slip faults. Isolated mountains: J- Jargalant Khayrkhan, B- Bumbat Khayrkhan, Bt- Baatar Khayrkhan, D- Dariv. Folded Cenozoic sediments are in two places near the western and southeastern flanks of the Dariv Range (Devyatkin, 1981; Khukhuudei et al., 2024). Main structure-bound faults are in numbered circles. I- Tsagaan Shuvuut, II- Khar Us Nuur, III- Khovd, IV- Tolbo Nuur, V- Tal Nuur, VI- Khoton, VII- Turgen, VIII- Bulgan, IX- Sharga, X- Khan Khukhey, continuation of Khangay fault. Intermontane depressions in the MAM are in Arabic numbers. One- Uureg Lake, 2- Achit Lake, 3- Uygar, 4- Tsagaan

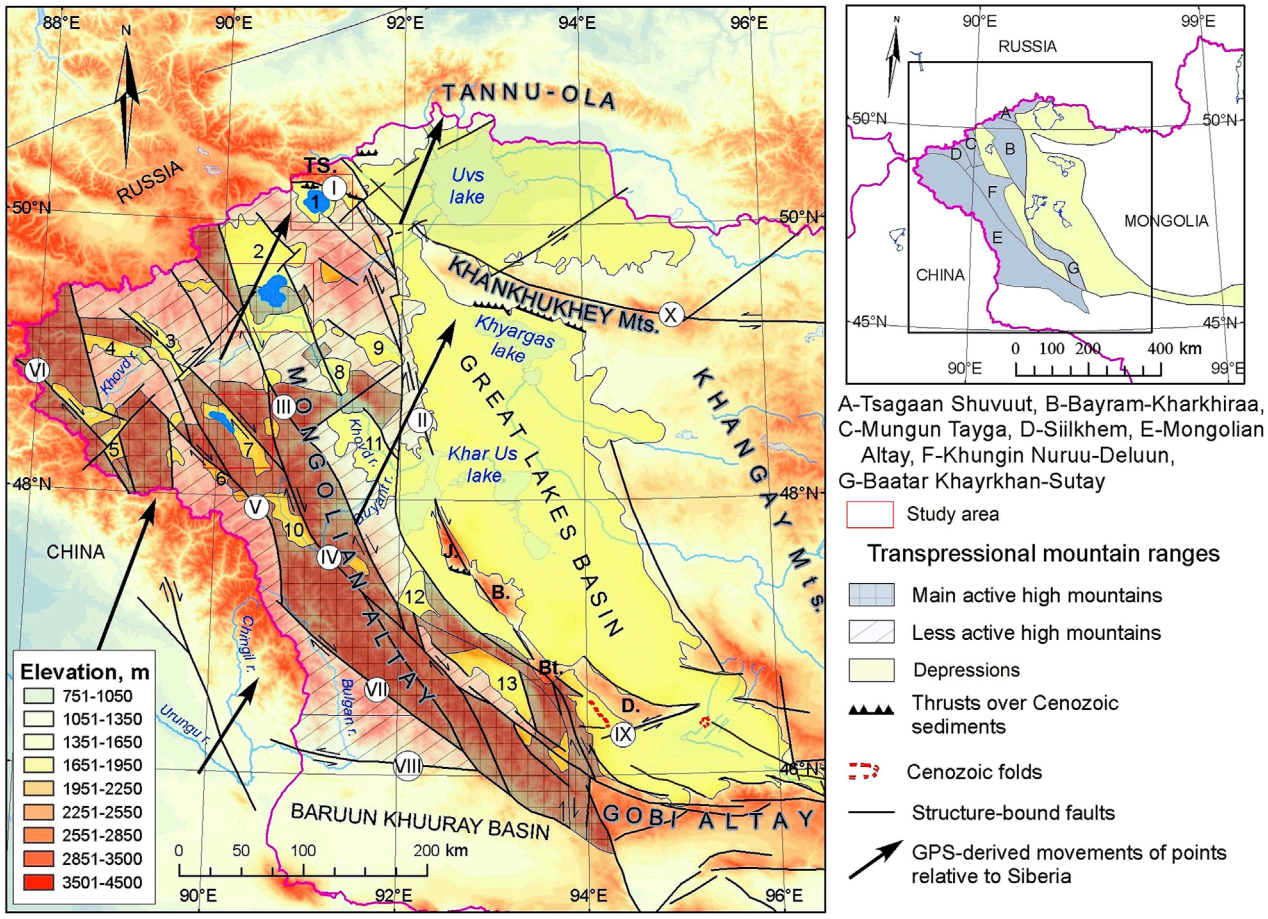

FIGURE 8
Neotectonic structures of the MAM (adapted from Khukhuudei et al., 2024).

Gol, 5- Upper Khovd, 6- Tal Nuur, 7- Tolbo Lake, 8-Middle Khovd, 9- Namir River, 10- Deluun, 11- Lower Khovd, 12- Mankhan, 13- Tsetseg (Khukhuudei et al., 2024). Black arrows represent GPS velocities of points relative to Siberia (data from Calais et al., 2003). The tectonic forces at play have influenced the distribution, size, and depth of these depressions. The study of fault lines, thrusts, and seismic activity in the area helps to understand how these features have evolved, as well as their role in the ongoing tectonic adjustments of the Altai Mountian. Areas of this study have been highlighted by the bright blue color.

The India-Asian collision has directly influenced the morphology, origin, and spatial pattern of lake depressions in Central Asia (Dobretsov et al., 1996; Faghih et al., 2012; Enkhbold et al., 2022c; Enkhbold et al., 2024a). The morphology of these lakes is additionally influenced by the region's climatic and hydrological conditions. The harsh continental climate, with its wide temperature variations and limited precipitation, has played a significant role in determining the shape and size of the lakes. In some cases, tectonic movements have influenced the hydrological systems, altering water levels and lake shapes (Figure 9).

The ongoing tectonic activity continues to reshape the land surface, causing changes in the elevation and morphology of the depressions. A critical aspect of studying the lake depressions in the Altai Mountains is understanding how tectonic forces interact with surface processes like erosion, sediment deposition, and climate change.

Faults influence the formation of areas where water is stored and accumulated. Water can be accumulated along the sides of faults or in sections along fault lines, leading to the formation of lakes. These lakes play a crucial role in the ecological balance of the region and have significant geomorphological importance. These depressions are associated with tectonic impact and are shaped by the interplay of uplift and subsidence along fault structures. Consequently, the morphology of lake basins undergoes continuous modification, influencing water levels and shoreline dynamics.

For example, seismic events can result in temporary fluctuations in lake water levels or even trigger the formation of new depressions. Erosion and sediment deposition, influenced by both tectonic uplift and climatic conditions, further modify the landscapes surrounding the lakes, adding another layer of complexity to the geomorphological study.

The study of these lake depressions offers valuable insights into the regional geodynamics of the Altai Mountains. Analyzing the tectonic and geomorphological characteristics of the depressions allows researchers to gain deeper insight into the mechanisms underlying the region's tectonic evolution. Additionally, these

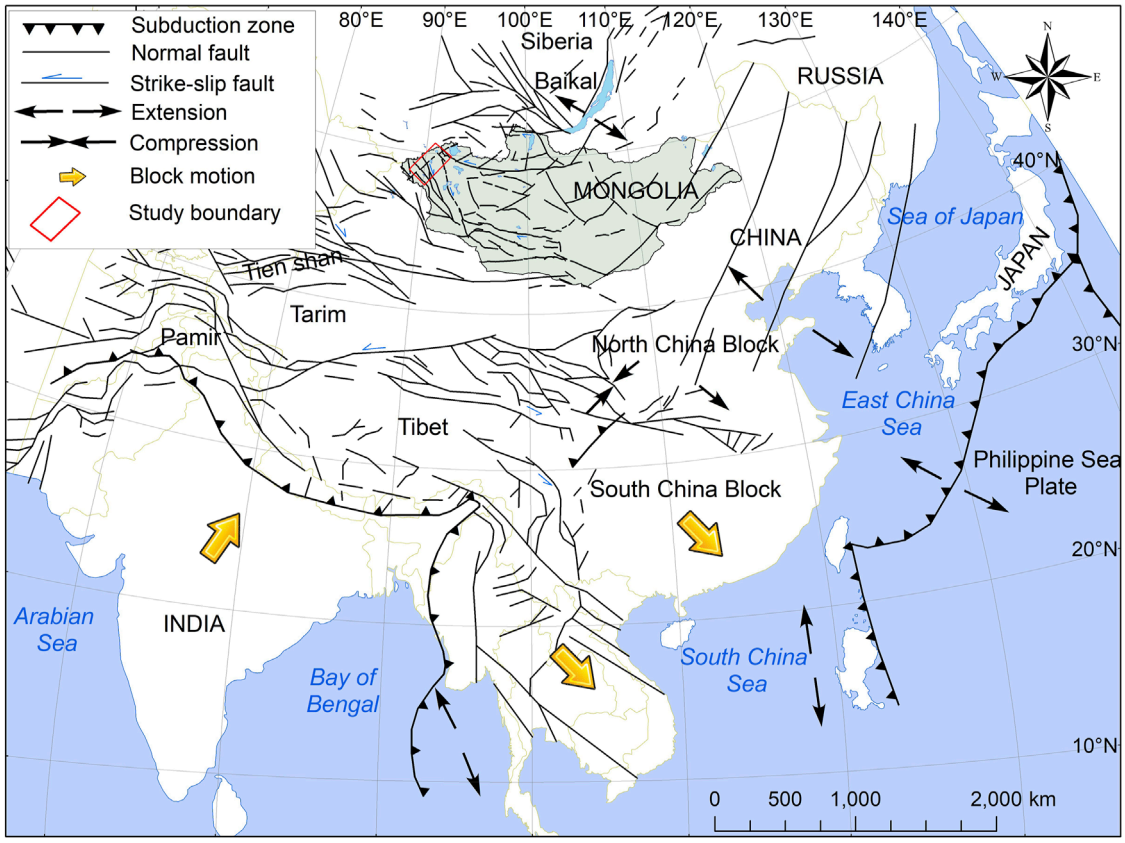

FIGURE 9
Structural-tectonic map illustrating Cenozoic continental deformation associated with the India-Asia collision, including the MAM fault system (modified after Molnar and Tapponnier, 1975; Tapponnier and Molnar, 1979).

studies can contribute to a broader understanding of the seismic hazards in the area and their potential impact on the environment and local communities.

The lakes also serve as natural archives, preserving sediment records that can be used to reconstruct past climatic conditions, seismic events, and tectonic movements. This multidisciplinary approach, integrating tectonics, geomorphology, and climate science, offers a comprehensive framework for understanding the geological history of the region.

The tectonic geomorphological study of the lake depressions in the Altai Mountains offers a fascinating window into the complex interplay between tectonic forces and surface processes. These depressions not only provide valuable insights into the region's geological history but also present a unique opportunity to examine the dynamic interplay between endogenic and exogenic Earth processes. Further research in this area can provide critical insights into the ongoing tectonic evolution of Central Asia and its implications for regional development and natural hazards.

6 Conclusion

The main characteristic of the depressions is that the Uureg, Achit, and Tolbo lakes are deep, well-defined, and developed along fault lines. By utilizing satellite imagery and morphometric indices to analyze their spatial distribution, researchers have identified a detailed understanding of the tectonic impact in these lake depressions.

Analysis of the HI (%) values for the MAM lake depressions is significantly high, indicating active tectonic movements in these regions. Furthermore, the Smf, Bs, RSl, and Re indices provide additional evidence of ongoing tectonic processes, with the observed values suggesting substantial fault activity and morphological changes along the major fault lines within these lake depressions.

Based on the regularity of the faults found in these depressions, it is confirmed that the lake depressions exhibit a tectonic origin. These depressions follow the major fault zones of tectonic uplift in the MAM, oriented from the southwest to the northeast.

The structural origins of the three lake depressions differ: Uureg Lake formed as a ramp basin, Achit Lake as a remnant low basin, and Tolbo Lake as a half-ramp basin. These basin types reflect distinct tectonic controls, including thrust faulting, strike-slip motion, and tilted thrust faulting. Lake depressions in MAM regions, formed by neotectonic processes related to the Indian - Eurasian plate collision, are bounded by major faults and exhibit active uplift and subsidence, making them prominent tectonic features of the landscape.

The tectonic and surface features observed in the depressions of lakes suggest that their origins are relatively similar, having formed under the same tectonic conditions of Mongolia, as well as the directional and transitional patterns of neotectonic movement.

Data availability statement

The datasets presented in this study can be found in online repositories. The names of the repository/repositories and accession number(s) can be found in the article/supplementary material. The satellite data supporting the conclusions of this article will be made available by the authors upon reasonable request.

Author contributions

AE: Conceptualization, Data curation, Formal Analysis, Investigation, Methodology, Resources, Software, Validation, Visualization, Writing – original draft. UK: Conceptualization, Data curation, Formal Analysis, Funding acquisition, Methodology, Project administration, Resources, Supervision, Visualization, Writing – original draft, Writing – review and editing. YBS: Formal Analysis, Funding acquisition, Investigation, Project administration, Software, Supervision, Validation, Visualization, Writing – original draft, Writing – review and editing. GY: Formal Analysis, Investigation, Methodology, Resources, Software, Visualization, Writing – review and editing. BBa: Data curation, Formal Analysis, Investigation, Methodology, Resources, Software, Validation, Writing – review and editing. DD: Conceptualization, Data curation, Formal Analysis, Funding acquisition, Project administration, Resources, Visualization, Writing – review and editing. SG: Data curation, Formal Analysis, Investigation, Methodology, Resources, Software, Visualization, Writing – review and editing. ST: Data curation, Formal Analysis, Resources, Software, Validation, Visualization, Writing – review and editing. BBo: Data curation, Formal Analysis, Investigation, Methodology, Resources, Software, Writing – review and editing. DB: Data curation, Formal Analysis, Investigation, Methodology, Resources, Software, Writing – review and editing. BG: Investigation, Methodology, Resources, Software, Validation, Visualization, Writing – review and editing.

Funding

The author(s) declare that financial support was received for the research and/or publication of this article. This work was conducted as part of the International Scholar Exchange Fellowship (ISEF) Program of the Chey Institute for Advanced Studies (2025–2026), in the Republic of Korea. Additionally, this work has been done within the framework of project (P2024-4824) supported by the National University of Mongolia.

Acknowledgments

We would like to express our gratitude to the editor Laura Suárez and the five reviewers for their invaluable comments and suggestions, which greatly contributed to the improvement of this manuscript.

Conflict of interest

The authors declare that the research was conducted in the absence of any commercial or financial relationships that could be construed as a potential conflict of interest.

Generative AI statement

The author(s) declare that no Generative AI was used in the creation of this manuscript.

Any alternative text (alt text) provided alongside figures in this article has been generated by Frontiers with the support of artificial intelligence and reasonable efforts have been made to ensure accuracy, including review by the authors wherever possible. If you identify any issues, please contact us.

Publisher's note

All claims expressed in this article are solely those of the authors and do not necessarily represent those of their affiliated organizations, or those of the publisher, the editors and the reviewers. Any product that may be evaluated in this article, or claim that may be made by its manufacturer, is not guaranteed or endorsed by the publisher.

References

Agatova, A. R., and Nepop, R. K. (2019). Pleistocene fluvial catastrophes in now arid NW areas of Mongolian Inland drainage basin. *Glob. Planet. Change* 175, 211–225. doi:10.1016/j.gloplacha.2019.02.009

Aher, P. D., Adinarayana, J., and Gorantiwar, S. D. (2014). Quantification of morphometric characterization and prioritization for management planning in semi-arid tropics of India: a remote sensing and GIS approach. *J. Hydrol.* 511, 850–860. doi:10.1016/j.jhydrol.2014.02.028

Anand, A. K., and Pradhan, S. P. (2019). Assessment of active tectonics from geomorphic indices and morphometric parameters in part of Ganga basin. *J. Mt. Sci.* 16 (8), 1943–1961. doi:10.1007/s11629-018-5172-2

Badarch, G., Cunningham, W. D., and Windley, B. F. (2002). A new terrane subdivision for Mongolia: implications for the Phanerozoic crustal growth of Central Asia. *J. Asian Earth Sci.* 21 (1), 87–110. doi:10.1016/S1367-9120(02)00017-2

Baljinnyam, I., Bayasgalan, A., Borisov, B. A., Cisternas, A., Dem'yanovich, M. G., Ganbaatar, L., et al. (1993). *Ruptures of major earthquakes and active deformation in Mongolia and its surroundings*, 181. Boulder, CO: Geological Society of America, 1–60. doi:10.1130/mem181-p1

Bayasgalan, A., Jackson, J., Ritz, J. F., and Carretier, S. (1999a). Field examples of strike-slip fault terminations in Mongolia and their tectonic significance. *Tectonics* 18 (3), 394–411. doi:10.1029/1999TC900007

Bayasgalan, A., Jackson, J., Ritz, J. F., and Carretier, S. (1999b). 'Forebergs', flower structures, and the development of large intra-continental strike-slip faults: the Gurvan Bogd fault system in Mongolia. *J. Struct. Geol.* 21 (10), 1285–1302. doi:10.1016/S0191-8141(99)00064-4

Bayasgalan, A., Jackson, J., and McKenzie, D. (2005). Lithosphere rheology and active tectonics in Mongolia: relations between earthquake source parameters, gravity and GPS measurements. *Geophys. J. Int.* 163 (3), 1151–1179. doi:10.1111/j.1365-246X.2005.02764.x

Bishop, M. P., James, L. A., Shroder Jr, J. F., and Walsh, S. J. (2012). Geospatial technologies and digital geomorphological mapping: concepts, issues and research. *Geomorphology* 137 (1), 5–26. doi:10.1016/j.geomorph.2011.06.027

Bucknam, R. C., and Anderson, R. E. (1979). Estimation of fault-scarp ages from a scarp-height–slope-angle relationship. *Geology* 7 (1), 11–14. doi:10.1130/0091-7613(1979)7<11:EOFAFA>2.0.CO;2

Bull, W. B., and McFadden, L. D. (1980). "Tectonic geomorphology north and south of the Garlock fault, California," in *Geomorphology in arid regions* (London, United Kingdom: Routledge), 115–138.

Calais, E., Vergnolle, M., San'Kov, V., Lukhnev, A., Miroshnitchenko, A., Amarjargal, S., et al. (2003). GPS measurements of crustal deformation in the Baikal-Mongolia area (1994–2002): implications for current kinematics of Asia. *J. Geophys. Res. Solid Earth.* 108 (B10). doi:10.1029/2002JB002373

Canty, M. J. (2019). *Image analysis, classification and change detection in remote sensing: with algorithms for Python*. Boca Raton, FL: Crc Press. doi:10.1201/9780429464348

Carson, B., Wegmann, K., and Center, G. (2008). *Quaternary tectonic and geomorphic evolution of the Deluun Nuruu, Mongolian altay, Western Mongolia*. London, United Kingdom: Keck Geology Consortium Research Proposal.

Chen, J., Wang, H., Liu, Y., Ma, S., and Huang, W. (2023). Temperature variations along the Silk Road over the past 2000 years: integration and perspectives. *Sci. China Earth Sci.* 66 (7), 1468–1477. doi:10.1007/s11430-022-1079-5

Chibani, A., Hadji, R., and Younes, H. (2022). A combined field and automatic approach for lithological discrimination in semi-arid regions, the case of geological maps of bir later region and its vicinity, Nementcha mounts, Algeria. *Geom. Landmanag. Landsc.* (4), 7–26. doi:10.15576/GLL/2022.4.7

Church, M. (2013). Refocusing geomorphology: field work in four acts. *Geomorphology* 200, 184–192. doi:10.1016/j.geomorph.2013.01.014

Cohen, A. S. (2003). *Paleolimnology: the history and evolution of lake systems*. New York, United States: Oxford University Press.

Conrad, O., Bechtel, B., Bock, M., Dietrich, H., Fischer, E., Gerlitz, L., et al. (2015). System for automated geoscientific analyses (SAGA) v.2.1.4. *Geosci. Model Dev.* 8 (7), 1991–2007. doi:10.5194/gmd-8-1991-2015

Copley, A., and McKenzie, D. (2007). Models of crustal flow in the India-Asia collision zone. *Geophys. J. Int.* 169 (2), 683–698. doi:10.1111/j.1365-246X.2007.03343.x

Cunningham, W. D. (1998). Lithospheric controls on late Cenozoic construction of the Mongolian Altai. *Tectonics* 17 (6), 891–902. doi:10.1029/1998TC900001

Cunningham, D. (2005). Active intracontinental transpressional mountain building in the Mongolian Altai: defining a new class of orogen. *Earth Planet. Sci. Lett.* 240 (2), 436–444. doi:10.1016/j.epsl.2005.09.013

Cunningham, W. D., Windley, B. F., Dorjnamjaa, D., Badamgarov, G., and Saandar, M. (1996). A structural transect across the Mongolian Western Altai: active transpressional mountain building in central Asia. *Tectonics* 15 (1), 142–156. doi:10.1029/95TC02354

Cunningham, D., Dijkstra, A., Howard, J., Quarles, A., and Badarch, G. (2003). Active intraplate strike-slip faulting and transpressional uplift in the Mongolian Altai. *Geol. Soc. Lond.* 210, 65–87. doi:10.1144/GSL.SP.2003.210.01.05

Das, B. C., Islam, A., and Sarkar, B. (2022). Drainage basin shape indices to understanding channel hydraulics. *Water Resour. Manag.* 36 (8), 2523–2547. doi:10.1007/s11269-022-03121-4

Davaasambuu, B., Ferry, M., Ritz, J. F., and Munkhuu, U. (2023). The Ar-Hötöl surface rupture along the Khovd fault (Mongolian Altay). *J. Maps* 19 (1), 2132884. doi:10.1080/17445647.2022.2132884

De Grave, J., Buslov, M. M., and Van den haute, P. (2007). Distant effects of India–Eurasia convergence and Mesozoic intracontinental deformation in Central Asia: constraints from apatite fission-track thermochronology. *J. Asian Earth Sci.* 29 (2-3), 188–204. doi:10.1016/j.jseaes.2006.03.001

Demberel, O., Dash, C., Dugersuren, B., Bayarmaa, M., Seong, Y. B., Chakraborty, E., et al. (2024). Flooding (or breaching) of inter-connected proglacial lakes by cascading overflow in the arid region of Western Mongolia (Mt. Tsambagarav, Mongolian Altai). *J. Mt. Sci.* 21 (10), 3215–3233. doi:10.1007/s11629-024-9054-5

Dergunov, A. B. (1989). *The Caledonides of the Central Asia, Transactions, 437. 192*. Moscow: Nauka.

Dergunov, A. B., Luvsandanzan, B., and Pavlenko, V. S. (1980). "Geology of west Mongolia," 31. Moscow: Nauka, 195.

Derikvand, S., and Farahpour, M. M. (2020). Assessment of relative active tectonic of the Khorramabad Basin using morphometric indices and fractal model analysis (Lorestan, north-west Zagros belt). *Quant. Geomorphol. Res.* 9 (3), 88–107. doi:10.22034/gmpj.2020.122216

Devyatkin, E. V. (1981). The Cenozoic of Inner Asia (stratigraphy, geochronology and correlation). *Trans. Jt. Soviet-Mongolian Scientific-Research Geol. Exped.* 27, 1–196.

Di Crescenzo, G., and Santo, A. (2005). Debris slides–rapid earth flows in the carbonate massifs of the Campania region (Southern Italy): morphological and morphometric data for evaluating triggering susceptibility. *Geomorphology* 66 (1-4), 255–276. doi:10.1016/j.geomorph.2004.09.015

Dietze, E., Wünnemann, B., Diekmann, B., Aichner, B., Hartmann, K., Herzschuh, U., et al. (2010). Basin morphology and seismic stratigraphy of Lake Donggi Cona, north-eastern Tibetan Plateau, China. *Quat. Int.* 218 (1-2), 131–142. doi:10.1016/j.quaint.2009.11.035

Dobretsov, N. L., Buslov, M. M., Delvaux, D., Berzin, N. A., and Ermikov, V. D. (1996). Meso-and Cenozoic tectonics of the Central Asian Mountain belt: effects of lithospheric plate interaction and mantle plumes. *Int. Geol. Rev.* 38 (5), 430–466. doi:10.1080/00206819709465345

El Hamdouni, R., Irigaray, C., Fernandez, T., Chacón, J., and Keller, E. A. (2008). Assessment of relative active tectonics, southwest border of the Sierra Nevada (Southern Spain). *Geomorphology* 96 (1-2), 150–173. doi:10.1016/j.geomorph.2007.08.004

Emanov, A. F., Emanov, A. A., Leskova, E. V., Kolesnikov, Y. I., Yankaitis, V. V., and Filina, A. G. (2012). The *Ms* = 7.0 Uureg Nuur earthquake of 15.05.1970 (Mongolian Altai): the aftershock process and current seismicity in the epicentral area. *Russ. Geol. Geophys.* 53 (10), 1090–1099. doi:10.1016/j.rgg.2012.08.009

Enkhbold, A., Khukhuudei, U., and Doljin, D. (2021). Morphological classification and origin of lake depressions in Mongolia. *Proc. Mong. Acad. Sci.* 61 (02), 35–43. doi:10.5564/pmas.v61i02.1758

Enkhbold, A., Khukhuudei, U., Kusky, T., Tsermaa, B., and Doljin, D. (2022a). Depression morphology of Bayan Lake, Zavkhan province, Western Mongolia: implications for the origin of lake depression in Mongolia. *Phys. Geogr.* 43 (6), 727–752. doi:10.1080/02723646.2021.1899477

Enkhbold, A., Dorjsuren, B., Khukhuudei, U., Yadamsuren, G., Bardarch, D., Dorjgochoo, S., et al. (2022b). Impact of faults on the origin of lake depressions: a case study of Bayan Nuur depression, North-west Mongolia, Central Asia. *Geogr. Fis. Dinam. Quat.* 44 (1), 53–66. doi:10.4461/GFDQ.2021.44.5

Enkhbold, A., Khukhuudei, U., Kusky, T., Chun, X., Yadamsuren, G., Ganbold, B., et al. (2022c). Morphodynamic development of the Terkhiin Tsagaan lake depression, Central Mongolia: implications for the relationships of faulting, volcanic activity, and lake depression formation. *J. Mt. Sci.* 19 (9), 2451–2468. doi:10.1007/s11629-021-7144-1

Enkhbold, A., Khukhuudei, U., and Doljin, D. (2022d). Review of modern trends and historical stages of development of lake research in Mongolia. *Proc. Mong. Acad. Sci.* 62 (01), 25–37. doi:10.5564/pmas.v62i01.2085

Enkhbold, A., Khukhuudei, U., Seong, Y. B., Gonchigjav, Y., Dingjun, L., and Ganbold, B. (2024a). Geomorphological study of the origin of Mongolian Altai Mountains Lake depressions: implications for the relationships between tectonic and glacial processes. *Mong. Geosci.* 29 (58), 1–18. doi:10.5564/mgs.v29i58.3237

Enkhbold, A., Dingjun, L., Ganbold, B., Yadamsuren, G., Tsasanchimeg, B., Dorligjav, S., et al. (2024b). Changes in morphometric parameters of lakes in different ecological zones of Mongolia: implications of climate change. *Clim. Res.* 92, 79–95. doi:10.3354/cr01734

Enkhbold, A., Khukhuudei, U., and Doljin, D. (2024c). New geomorphological districts of lakes in Mongolia. *MJGG* 61 (45), 1–18. doi:10.5564/mjgg.v61i45.3235

Enkhbold, A., Vandansambuu, B., Yadamsuren, G., Dorjsuren, B., Dorligjav, S., Gonchigjav, Y., et al. (2025a). Estimation of morphometric parameters of lakes based on satellite imagery data: implications of relationships between lakes in the arid region of western Mongolia, Central Asia. *Quaest. Geogr.* 44 (1), 21–38. doi:10.14746/quageo-2025-0002

Enkhbold, A., Khukhuudei, U., Seong, Y. B., Badarch, D., Tsedevdorj, S. O., Batbold, B., et al. (2025b). Impact of faulting on the depression morphology of Ulaagchinii Khar Lake in Mongolia. *Mong. Geosci.* 30 (61), 14–32. doi:10.5564/mgs.v30i61.3855

Ezati, M., Gholami, E., and Mousavi, S. M. (2021). Tectonic activity level evaluation using geomorphic indices in the Shekarab Mountains, Eastern Iran. *Arab. J. Geosci.* 14, 385–16. doi:10.1007/s12517-021-06724-0

Faghih, A., Samani, B., Kusky, T., Khabazi, S., and Roshanak, R. (2012). Geomorphologic assessment of relative tectonic activity in the Maharlou Lake Basin, Zagros Mountains of Iran. *Geol. J.* 47 (1), 30–40. doi:10.1002/gj.1329

Farhan, Y., and Anaba, O. (2016). Flash flood risk estimation of Wadi Yutum (Southern Jordan) watershed using GIS based morphometric analysis and remote sensing techniques. *Open J. Mod. Hydrol.* 6 (02), 79–100. doi:10.4236/ojmh.2016.62008

Farhan, Y., Elgaziri, A., Elmaji, I., and Ali, I. (2016a). Hypsometric analysis of Wadi Mujib-Wala watershed (Southern Jordan) using remote sensing and GIS techniques. *Int. J. Geosci.* 7 (02), 158–176. doi:10.4236/ijg.2016.72013

Farhan, Y., Mousa, R., Dagarah, A., and Shtaya, D. (2016b). Regional hypsometric analysis of the Jordan Rift drainage basins (Jordan) using Geographic Information System. *Open J. Geol.* 6 (10), 1312–1343. doi:10.4236/ojg.2016.610096

Filosofov, V. P. (1967). "*The value of the map of potential relief energy for geomorphological and neotectonic studies*" in Science. *Sib. Department. Methods geomorphological*, 193–198.

Florinsky, I. V. (1996). Quantitative topographic method of fault morphology recognition. *Geomorphology* 16 (2), 103–119. doi:10.1016/0169-555X(95)00136-S

Gallant, J. C., and Dowling, T. I. (2003). A multiresolution index of valley bottom flatness for mapping depositional areas. *Water Resour. Res.* 39 (12). doi:10.1029/2002WR001426

Ganas, A., Pavlides, S., and Karastathis, V. (2005). DEM-based morphometry of range-front escarpments in Attica, central Greece, and its relation to fault slip rates. *Geomorphology* 65 (3-4), 301–319. doi:10.1016/j.geomorph.2004.09.006

Gavrilova, S. P. (1975). "Granitoid formations of western Mongolia," in *In granitoid and alkaline formations in the structures of western and northern Mongolia* (Moscow, Nauka: Transactions), 50–143.

Ghafor, I. M. (2022). Systematic, microbiostratigraphy and paleo-ecology of the Bajwan Formation (Late Oligocene) in the Kirkuk Well-160, northeastern Iraq. *Carbonates Evaporites* 37 (3), 45–18. doi:10.1007/s13146-022-00793-2

Ghafor, I. M., and Ahmad, P. M. (2021). Stratigraphy of the Oligocene-Early Miocene successions, Sangaw area, Kurdistan Region, NE-Iraq. *Arab. J. Geosci.* 14 (6), 454. doi:10.1007/.s12517-021-06697-0

Ghafor, I. M., Ahmad, P., and Khafaf, A. A. (2023). Biostratigraphy and paleoecology of the Anah Formation in Kurdistan Region, Iraq. *Iraqi Bull. Geol. Min.* 19 (1), 17–28. doi:10.59150/ibgm1901a02

Green, R., and White, S. (2019). "Evaluating geomorphological criteria in temperate zones: a case study," in *Proc. Int. Geomorphol. Conf.* Editors P. Black, and J. White (Springer), 200–215. doi:10.1007/978-3-030-22593-4_12

Grohmann, C. H. (2018). Evaluation of TanDEM-X DEMs on selected Brazilian sites: Comparison with SRTM, ASTER GDEM and ALOS AW3D30. *Remote Sens. Environ.* 212, 121–133. doi:10.1016/j.rse.2018.04.043

Grohmann, C. H., Riccomini, C., and Alves, F. M. (2007). SRTM-based morphotectonic analysis of the Puna Plateau, Central Andes. *Comput. Geosci.* 33 (8), 1107–1116. doi:10.1016/j.cageo.2006.05.002

Grunert, J., Lehmkuhl, F., and Walther, M. (2000). Paleoclimatic evolution of the Uvs Nuur basin and adjacent areas (Western Mongolia). *Quat. Int.* 65, 171–192. doi:10.1016/S1040-6182(99)00043-9

Gürbüz, A., and Gürer, Ö. F. (2008). Tectonic geomorphology of the North Anatolian fault zone in the lake Sapanca Basin (eastern Marmara Region, Turkey). *Geosci. J.* 12, 215–225. doi:10.1007/s12303-008-0022-9

Ha, S., Seong, Y. B., and Son, M. (2023). Tectonic geomorphology and Quaternary fault slip rates in the Tsambagarav Massif, Mongolian Altai. *Earth Surf. Process. Landforms* 48 (7), 1428–1449. doi:10.1002/esp.5558

Hassen, M. B., Deffontaines, B., and Turki, M. M. (2014). Recent tectonic activity of the Gafsa fault through morphometric analysis: Southern Atlas of Tunisia. *Quat. Int.* 338, 99–112. doi:10.1016/j.quaint.2014.05.009

Hooper, D. M., Bursik, M. I., and Webb, F. H. (2003). Application of high-resolution, interferometric DEMs to geomorphic studies of fault scarps, Fish Lake Valley, Nevada–California, USA. *Remote Sens. Environ.* 84 (2), 255–267. doi:10.1016/S0034-4257(02)00110-4

Howard, J. P., Cunningham, W. D., Davies, S. J., Dijkstra, A. H., and Badarch, G. (2003). The stratigraphic and structural evolution of the Dzereg Basin, western Mongolia: clastic sedimentation, transpressional faulting and basin destruction in an intraplate, intracontinental setting. *Basin Res.* 15 (1), 45–72. doi:10.1046/j.1365-2117.2003.00198.x

Hu, Y., Huang, X., Demberel, O., Zhang, J., Xiang, L., Gundegmaa, V., et al. (2024). Quantitative reconstruction of precipitation changes in the Mongolian Altai Mountains since 13.7 ka. *Catena* 234, 107536. doi:10.1016/j.catena.2023.107536

Huang, X., Peng, W., Rudaya, N., Grimm, E. C., Chen, X., Cao, X., et al. (2018). Holocene vegetation and climate dynamics in the Altai Mountains and surrounding areas. *Geophys. Res. Lett.* 45 (13), 6628–6636. doi:10.1029/2018GL078028

Huang, C., Huang, X., Li, J., Wang, L., Jiang, L., Xiang, L., et al. (2024). Western Mongolian Plateau exhibits increasing Holocene temperature. *Glob. Planet. Change* 242, 104577. doi:10.1016/j.gloplacha.2024.104577

Hughes, P. D. (2010). Geomorphology and Quaternary stratigraphy: the roles of morpho-litho-and allostratigraphy. *Geomorphology* 123 (3-4), 189–199. doi:10.1016/j.geomorph.2010.07.025

Izokh, A. E., Vishnevskii, A. V., Polyakov, G. V., Kalugin, V. M., Oyunchimeg, T., Shelepaev, R. A., et al. (2010). The Ureg Nuur Pt-bearing volcanoplutonic picrite–basalt association in the Mongolian Altay as evidence for a Cambrian–Ordovician Large Igneous Province. *Russ. Geol. Geophys.* 51 (5), 521–533. doi:10.1016/j.rgg.2010.04.003

Izokh, A. E., Vishnevskii, A. V., Polyakov, G. V., and Shelepaev, R. A. (2011). Age of picrite and picrodolerite magmatism in western Mongolia. *Russ. Geol. Geophys.* 52 (1), 7–23. doi:10.1016/j.rgg.2010.12.002

Jacques, P. D., Salvador, E. D., Machado, R., Grohmann, C. H., and Nummer, A. R. (2014). Application of morphometry in neotectonic studies at the eastern edge of the Paraná Basin, Santa Catarina State, Brazil. *Geomorphology* 213, 13–23. doi:10.1016/j.geomorph.2013.12.037

Jolivet, M., Labaume, P., Monié, P., Brunel, M., Arnaud, N., and Campani, M. (2007). Thermochronology constraints for the propagation sequence of the south pyrenean basement thrust system (France-Spain). *Tectonics* 26 (5). doi:10.1029/2006TC002080

Jones, B. M., Grosse, G., Farquharson, L. M., Roy-Léveillée, P., Veremeeva, A., Kanevskiy, M. Z., et al. (2022). Lake and drained lake basin systems in lowland permafrost regions. *Nat. Rev. Earth Environ.* 3 (1), 85–98. doi:10.1038/s43017-021-00238-9

Jordan, G. (2003). Morphometric analysis and tectonic interpretation of digital terrain data: a case study. *Earth Surf. Process. Landforms* 28 (8), 807–822. doi:10.1002/esp.469

Kaufmann, A. (1975). *Introduction to the theory of fuzzy subsets*. New York: Academic Press.

Keller, E. A., and Pinter, N. (2002). *Active tectonics: Earthquakes, uplift, and landscape*. Upper Saddle River, NJ: Prentice Hall.

Khil'ko, S. D., and Kurushin, R. A. (1982). "Mongolian altay," in *Geomorphology of the people's republic of Mongolia, Trans* (Moscow: Nauka), 28, 40–54.

Khukhuudei, U., Kusky, T., Otgonbayar, O., and Wang, L. (2020). The early palaeozoic mega-thrusting of the Gondwana-derived Altay-Lake zone in Western Mongolia: implications for the development of the Central Asian orogenic belt and Paleo-Asian ocean evolution. *Geol. J.* 55 (3), 2129–2149. doi:10.1002/gj.3753

Khukhuudei, U., Kusky, T., Windley, B. F., Otgonbayar, O., and Wang, L. (2022). Ophiolites and ocean plate stratigraphy (OPS) preserved across the Central Mongolian Microcontinent: a new mega-archive of data for the tectonic evolution of the Paleo-Asian Ocean. *Gondwana Res.* 105, 51–83. doi:10.1016/j.gr.2021.12.008

Khukhuudei, U., Kusky, T., Windley, B. F., Otgonbayar, O., Wang, L., Nie, J., et al. (2024). Cenozoic intracontinental tectonics of Mongolia and its climate effects: a synthesized review. *Earth-Sci. Rev.* 258, 104934. doi:10.1016/j.earscirev.2024.104934

Klinge, M., Schluetz, F., Zander, A., Huelle, D., Batkhishig, O., and Lehmkuhl, F. (2021). Late Pleistocene lake level, glaciation and climate change in the Mongolian Altay deduced from sedimentological and palynological archives. *Quat. Res.* 99, 168–189. doi:10.1017/qua.2020.67

Korzhenkov, A. M., Usmanova, M. T., Anarbaev, A. A., Maksudov, F. A., Murudaliev, R. K., Zakhidov, T. K., et al. (2019). Underestimated seismic hazard of the Ferghana Depression: new archeoseismological data. *Izv. Atmos. Ocean. Phys.* 55, 1536–1546. doi:10.1134/S0001433819100062

Kot, R. (2018). A comparison of results from geomorphological diversity evaluation methods in the Polish Lowland (Toruń Basin and Chełmno Lakeland). *Geogr. Tidsskr.-Danish J. Geogr.* 118 (1), 17–35. doi:10.1080/00167223.2017.1343673

Kusky, T. M., Polat, A., Windley, B. F., Burke, K. C., Dewey, J. F., Kidd, W. S. F., et al. (2016). Insights into the tectonic evolution of the North China Craton through comparative tectonic analysis: a record of outward growth of Precambrian continents. *Earth-Sci. Rev.* 162, 387–432. doi:10.1016/j.earscirev.2016.09.002

Laurie, A., Jamsranjav, J., van den Heuvel, O., and Nyamjav, E. (2010). Biodiversity conservation and the ecological limits to development options in the Mongolian Altai: formulation of a strategy and discussion of priorities. *Cent. Asian Surv.* 29 (3), 321–343. doi:10.1080/02634937.2010.528188

Leeder, M. R. (2011). Tectonic sedimentology: sediment systems deciphering global to local tectonics. *Sedimentology* 58 (1), 2–56. doi:10.1111/j.1365-3091.2010.01207.x

Lehmkuhl, F. (2016). Modern and past periglacial features in Central Asia and their implication for paleoclimate reconstructions. *Prog. Phys. Geogr.* 40 (3), 369–391. doi:10.1177/0309133315615778

Lehmkuhl, F., and Lang, A. (2001). Geomorphological investigations and luminescence dating in the southern part of the Khangay and the Valley of the Gobi Lakes (Central Mongolia). *J. Quat. Sci.* 16 (1), 69–87. doi:10.1002/1099-1417(200101)16:1<69::aid-jqs583>3.0.co;2-o

Lehmkuhl, F., Grunert, J., Hülle, D., Batkhishig, O., and Stauch, G. (2018a). Paleolakes in the gobi region of southern Mongolia. *Quat. Sci. Rev.* 179, 1–23. doi:10.1016/j.quascirev.2017.10.035

Lehmkuhl, F., Nottebaum, V., and Hülle, D. (2018b). Aspects of late Quaternary geomorphological development in the Khangai Mountains and the Gobi Altai Mountains (Mongolia). *Geomorphology* 312, 24–39. doi:10.1016/j.geomorph.2018.03.029

Lehmkuhl, F., Wolf, D., Boemke, B., Klinge, M., Batkhishig, O., and Grunert, J. (2024). Aeolian sediments in western Mongolia: distribution and (paleo) climatic implications. *Geomorphology* 465, 109407. doi:10.1016/j.geomorph.2024.109407

Lehner, B. (2024). "Rivers and Lakes—Their distribution, origins, and forms," in *Wetzel's limnology* (Academic Press), 25–56.

Li, Y., Liu, X., Wang, W., Xiang, L., Hu, Y., Jeppesen, E., et al. (2025). Lateglacial and Holocene hydroclimatic variability documented by Cladocera of Tolbo Lake in the Altai Mountains, western Mongolia. *Quat. Sci. Rev.* 351, 109186. doi:10.1016/j.quascirev.2025.109186

Malins, D., and Metternicht, G. (2006). Assessing the spatial extent of dryland salinity through fuzzy modeling. *Ecol. Model.* 193 (3-4), 387–411. doi:10.1016/j.ecolmodel.2005.08.044

Maliqi, E., Kumar, N., Latifi, L., and Singh, S. K. (2023). Soil erosion estimation using an empirical model, hypsometric integral and geo-information science–a case study. *Ecol. Eng. Environ. Technol.* 24, 62–72. doi:10.12912/27197050/161957

Manchar, N., Hadji, R., Bougherara, A., and Boufaa, K. (2022). Assessment of relative-active tectonics in rhumel-smendou basin (ne algeria)–observations from the morphometric indices and hydrographic features obtained by the digital elevation model. *Geom. Landmanag. Landsc.* (4), 47–65. doi:10.15576/GLL/2022.4.47

Molnar, P., and Tapponnier, P. (1975). Cenozoic Tectonics of Asia: effects of a Continental Collision: features of recent continental tectonics in Asia can be interpreted as results of the India-Eurasia collision. *Science* 189 (4201), 419–426. doi:10.1126/science.189.4201.419

Nissen, E., Walker, R. T., Bayasgalan, A., Carter, A., Fattahi, M., Molor, E., et al. (2009a). The late Quaternary slip-rate of the har-us-nuur fault (Mongolian Altai) from cosmogenic 10Be and luminescence dating. *EPSL* 286 (3-4), 467–478. doi:10.1016/j.epsl.2009.06.048

Nissen, E., Walker, R., Molor, E., Fattahi, M., and Bayasgalan, A. (2009b). Late Quaternary rates of uplift and shortening at Baatar Hyarhan (Mongolian Altai) with optically stimulated luminescence. *Geophys. J. Int.* 177 (1), 259–278. doi:10.1111/j.1365-246X.2008.04067.x

Nixon, M., and Aguado, A. (2019). *Feature extraction and image processing for computer vision*. Academic Press.

Nottebaum, V., Stauch, G., van der Wal, J. L., Zander, A., Schlütz, F., Shumilovskikh, L., et al. (2022). Late Quaternary landscape evolution and paleoenvironmental implications from multiple geomorphic dryland systems, Orog Nuur Basin, Mongolia. *Earth Surf. Process. Landf.* 47 (1), 275–297. doi:10.1002/esp.5247

Onorato, M. R., Coronato, A., Perucca, L. P., Rabassa, J., and López, R. (2017). Morpho-bathymetry and surficial morphology of Udaeta Lake, along the Magallanes-Fagnano fault system, Tierra del Fuego, Argentina. *J. South Am. Earth Sci.* 76, 1–10. doi:10.1016/j.jsames.2017.02.001

Oyunchimeg, T., and Narantsetseg, T. (2020). The lithology and inorganic geochemistry from Achit Lake sediments as an indicator of paleoclimatic change, Western Mongolia. *Trans. Jpn. Geomorphol. Union* 41 (3), 249–259. doi:10.60380/tjgu.41.3_249

Pinter, N., and Keller, E. A. (1995). Geomorphological analysis of neotectonic deformation, northern Owens Valley, California. *Geol. Rundsch* 84, 200–212. doi:10.1007/BF00192251

Pournamdari, M., Hashim, M., and Pour, A. B. (2014). Application of ASTER and landsat TM data for geological mapping of esfandagheh ophiolite complex, Southern Iran. *Resour. Geol.* 64, 233–246. doi:10.1111/rge.12038

Rahimzadeh, N., Wolf, D., Tsukamoto, S., Frechen, M., and Lehmkuhl, F. (2025). Luminescence dating of palaeoshoreline deposits from Khyargas Nuur, Western Mongolia: a comparative study of multigrain and single-grain K-feldspar dating. *J. Quat. Sci.* 40, 1043–1055. doi:10.1002/jqs.3731

Ramel, F., Ritz, J. F., Ferry, M., Malcles, O., Davaasambuu, B., Arzhannikova, A. V., et al. (2025). Inframillimetric slip rate and~ 8kyr long recurrence intervals for Mw≥ 7.5 earthquakes along the southern section of the har-us-nuur fault (Mongolian Altay). *BSGF-EARTH Sci. B* 196, 8. doi:10.1051/bsgf/2025001

Ramírez-Herrera, M. T. (1998). Geomorphic assessment of active tectonics in the Acambay Graben, Mexican volcanic belt. *Earth Surf. Process. Landforms* 23 (4), 317–332. doi:10.1002/(sici)1096-9837(199804)23:4<317::aid-esp845>3.0.co;2-v

Rashidi, R. F., Ghafor, I. M., and Javadova, A. (2023). "Benthic Foraminifera as a tool for indication biostratigraphy and paleoecology of the Guri member (Mishan Formation), Bander Abbas, South Iran," *Mater. VII Int. Sci. Pract. Conf.*, 1, 37–53.

Roberts, D. W., Walker, J., and Dowling, T. I. (1997). *FLAG: a fuzzy landscape analysis GIS method for dryland salinity assessment*. Canberra, ACT: CSIRO Land and Water, 121–125.

Schallenberg, M., de Winton, M. D., Verburg, P., Kelly, D. J., Hamill, K. D., and Hamilton, D. P. (2013). "*Ecosystem services of lakes*,". New Zealand: Manaaki Whenua Press, 203–225.

Silva, P. G., Goy, J. L., Zazo, C., and Bardaji, T. (2003). Fault-generated Mountain fronts in southeast Spain: geomorphologic assessment of tectonic and seismic activity. *Geomorphology* 50 (1-3), 203–225. doi:10.1016/S0169-555X(02)00215-5

Singh, T. (2008). Tectonic implications of geomorphometric characterization of watersheds using spatial correlation: mohand Ridge, NW Himalaya, India. *Z Geomorphol.* 52 (4), 489–501. doi:10.1127/0372-8854/2008/0052-0489

Singh, T., Awasthi, A. K., and Caputo, R. (2012). The sub-Himalayan fold-thrust belt in the 1905 Kangra earthquake zone: a critical taper model perspective for seismic hazard analysis. *Tectonics* 31 (6). doi:10.1029/2012TC003120

Smith, J. (2020). Geomorphological criteria interpretation in arid regions. *J. Geomorphol.* 45 (2), 123–134. doi:10.1016/j.geomorph.2020.03.001

Strahler, A. N. (1952). Hypsometric (area-altitude) analysis of erosional topography. *Geol. Soc. Am. Bull.* 63 (11), 1117–1142. doi:10.1130/0016-7606(1952)63[1117:HAAOET]2.0.CO;2

Strahler, A. N. (1964). Quantitative geomorphology of drainage basins and channel networks. *Handb. Appl. Hydrol.* 4, 39–76. doi:10.4236/ijg.2016.72012

Strand, P. D., Putnam, A. E., Sambuu, O., Putnam, D. E., Denton, G. H., Schaefer, J. M., et al. (2022). A^{10}Be Moraine chronology of the last glaciation and termination at 49°N in the Mongolian Altai of central Asia. *Paleoceanogr. Paleoclimatol.* 37 (5), e2022PA004423. doi:10.1029/2022PA004423

Sun, A., Feng, Z., Ran, M., and Zhang, C. (2013). Pollen-recorded bioclimatic variations of the last ~ 22,600 years retrieved from Achit Nuur core in the western Mongolian Plateau. *Quat. Int.* 311, 36–43. doi:10.1016/j.quaint.2013.07.002

Taib, H., Hadji, R., Hamed, Y., Bensalem, M. S., and Amamria, S. (2024). Exploring neotectonic activity in a semiarid basin: a case study of the Ain Zerga watershed. *J. Umm Al-Qura Univ. Appl. Sci.* 10 (1), 20–33. doi:10.1007/s43994-023-00072-3

Tamani, F., Hadji, R., Hamad, A., and Hamed, Y. (2019). Integrating remotely sensed and GIS data for the detailed geological mapping in semi-arid regions: case of Youks les Bains Area, Tebessa Province, NE Algeria. *Geotech. Geol. Eng.* 37 (4), 2903–2913. doi:10.1007/s10706-019-00807-2

Tapponnier, P., and Molnar, P. (1979). Active faulting and Cenozoic tectonics of the Tien Shan, Mongolia, and Baykal regions. *J. Geophys. Res. Solid Earth* 84 (B7), 3425–3459. doi:10.1029/JB084iB07p03425

Theilen-Willige, B., Aher, S. P., Gawali, P. B., and Venkata, L. B. (2016). Seismic hazard analysis along Koyna Dam area, western Maharashtra, India: a contribution of remote sensing and GIS. *Geosciences* 6 (2), 20. doi:10.3390/geosciences6020020

Tomurtogoo, O. (2014). "Tectonics of Mongolia," in *Tectonics of northern, central and eastern Asia, explanatory note to the tectonic map of northern central eastern Asia and adjacent areas at scale 1:2500000*, 110–126.

Trifonov, V. G., Sokolov, S. A., Ovsyuchenko, A. N., Sokolov, S. Y., Batsaikhan, T., Demberel, S., et al. (2024). Active faults of Northern Central Mongolia, their correlation with neotectonics and deep structure of the Region. *Geotectonics* 58 (2), 149–176. doi:10.1134/S0016852124700109

Tsedevdorj, S. O. (2019). "Basic characteristics of the mountain landscapes of Mongolian Altay, issues of utilization and protection,". *Dr. Diss. Geogr. Sci.*, 170.

Tsedevdorj, S. O., Khurelbaatar, T., Ganbold, U., Yadamsuren, G., Avkhinsukh, A., Erkhembayar, B., et al. (2025). Climate change impact of land cover changes in the Kharhiraa-Turgen mountain region. *Mong. Geosci.* 30 (61), 1–13. doi:10.5564/mgs.v30i61.3866

Tserensodnom, J. (1971). Lakes of Mongolia. *Mong. Acad. Sci. Inst. Geogr. Permafr. Ulaanbaatar, Mong.*, 78–103.

Tserensodnom, J. (2000). Catalog of lakes of Mongolia. *Mong. Acad. Sci. Inst. Geogr. Permafr. Ulaanbaatar, Mong. in Mong.*, 45–84.

Vijayarani, S., and Vinupriya, M. (2013). Performance analysis of canny and sobel edge detection algorithms in image mining. *Int. J. Innov. Res. Comput. Commun. Eng.* 1 (8), 1760–1767.

Walker, R. T., Bayasgalan, A., Carson, R., Hazlett, R., McCarthy, L., Mischler, J., et al. (2006). Geomorphology and structure of the Jid right-lateral strike-slip fault in the Mongolian Altay mountains. *J. Struct. Geol.* 28 (9), 1607–1622. doi:10.1016/j.jsg.2006.04.007

Walker, R. T., Nissen, E., Molor, E., and Bayasgalan, A. (2007). Reinterpretation of the active faulting in central Mongolia. *Geology* 35 (8), 759–762. doi:10.1130/G23716A.1

Walther, M., Kamp, U., Nandintsetseg, N. O., Dashtseren, A., and Temujin, K. (2024). Glacial Lakes of Mongolia. *Geographies* 4 (1), 21–39. doi:10.3390/geographies4010002

Whipple, K. X., and Gasparini, N. M. (2014). Tectonic control of topography, rainfall patterns, and erosion during rapid post–12 Ma uplift of the Bolivian Andes. *Lithosphere* 6 (4), 251–268. doi:10.1130/L325.1

Wolf, D., Lehmkuhl, F., Schaubert, V., Rahimzadeh, N., Frechen, M., Stauch, G., et al. (2025). Drivers of late Quaternary lake level fluctuations of Khyargas Nuur, western Mongolia-glacial meltwater discharge or atmospheric moisture supply? *Quat. Sci. Rev.* 359, 109373. doi:10.1016/j.quascirev.2025.109373

Yarmolyuk, V. V., Kovach, V. P., Kovalenko, V. I., Salnikova, E. B., Kozlovskii, A. M., Kotov, A. B., et al. (2011). Composition, sources, and mechanism of continental crust growth in the Lake Zone of the Central Asian Caledonides: I. Geological and geochronological data. *Petrology* 19, 55–78. doi:10.1134/S0869591111010085

Yembuu, B. (2021). "Climate and climate change of Mongolia," in *The physical geography of Mongolia* (Cham: Springer International Publishing), 51–76. doi:10.1007/978-3-030-61434-8_4

Zhang, C. (2012). Holocene hydrological change in western Mongolia inferred from the lake record of Achit Nuur. *Quat. Int.* 279, 557. doi:10.1016/j.quaint.2012.08.2065

Zhang, Y., Mao, C., Zhang, J., Huang, X., and Otgonbayar, D. (2023). Aeolian activities in the NW Mongolia during the Holocene recorded by grain-sizesensitive particles in the sediments of Lake Tolbo. *J. Lake Sci.* 35, 368–380. doi:10.18307/2023.0129

Zhang J, J., Huang, X., Qiang, M., Demberel, O., Wang, W., Zheng, M., et al. (2022). Increasing spring insolation in the Late Holocene intensified aeolian activity in dryland Asia. *Geophys. Res. Lett.* 49 (24), e2022GL101777. doi:10.1029/2022GL101777

Zhang S, S., Zhao, H., Sheng, Y., Chen, S., Li, G., and Chen, F. (2022). Late Quaternary lake level record of Orog Nuur, southern Mongolia, revealed by optical dating of paleo-shorelines. *Quat. Geochronol.* 72, 101370. doi:10.1016/j.quageo.2022.101370